Table 1. Acetaldehyde-derived DNA Adducts in *ALDH2*-deficient Alcoholics[4]

Acetaldehyde-derived DNA adducts	*ALDH2* Genotype		*p*-Value
	(*1/*1) [n=19] (Normal type)	(*1/*2) [n=25] (Deficient type)	
N^2-Ethyl-dG	17.8±15.9	130±52	0.03
α-S-Me-γ-OH-PdG	42.9±6.0	92.4±12.9	0.01
α-R-Me-γ-OH-PdG	61.3±6.4	114±15	0.02

Values are means±standard error of the mean (fmol/μM dG).
p-Values were calculated by the Wilcoxon–Mann–Whitney test (N^2-ethyl-dG) and *t*-test (α-Me-γ-OH-PdG).

Table 2. Stomach DNA Adduct Levels in Control and Alcohol-treated Mice Having Different *Aldh2* Genotypes[5]

	Aldh2 Genotype	n	N^2-Ethylidene dG level (adducts/10^7 bases)
Water	+/+	5	3.1±2.3
	+/−	6	2.0±0.6
	−/−	5	2.2±0.4
20% Ethanol	+/+	6	4.8±2.6
	+/−	5	7.9±1.1
	−/−	4	48.6±12.0

Values are means±standard error of the mean.
Mice were fed with water or 20% ethanol for 5 weeks.

日本人の約半数はこの酵素が欠損していて，体内にアセトアルデヒドが蓄積しやすい．アセトアルデヒドは DNA 損傷性や突然変異原性をもつ化合物なので，フラッシャー，すなわち *ALDH2* 欠損者では DNA 損傷が蓄積した結果，がんのリスクが高くなるのではないかと考えられてきた．アセトアルデヒドにより生成する DNA 付加体の構造を Fig. 2 に示す．久里浜病院の横山　顕先生の協力を得てアルコール依存症患者の血液中 DNA の分析を行ったところ，Table 1 に示すように *ALDH2* 欠損者に DNA 付加体が蓄積していることが明らかになった[4]．また，Table 2 は正常マウスおよび *Aldh2* ノックアウトマウスに 20% エタノールを 5 週間与えたときの，胃中の DNA 付加体 (N^2-ethylidine-dG, 還元して N^2-ethyl-dG として測定) を定量したものである．*Aldh2* +/+ は正常型，+/− はヘテロ欠損型，−/− はホモ欠損型である．飲酒したマウスでは，水を与えたマウスに比べて DNA 付加体が増えており，さらに *Aldh2* の遺伝子多型によって付加体数が劇的に変わっているのがわかる[5]．つまり，お酒の弱い人は，お酒を飲むと胃の DNA にダメージを受けやすいことがわかる．

5. DNA アダクトーム解析—生体内には何種類くらいの DNA 付加体が存在するのか？—

筆者は LC/MS/MS を用いて，既知 DNA 付加体の定量解析をするだけではなく，生体内の DNA 付加体を網羅的に解析する手法を開発してきた．この方法をプロテオームやメタボロームをもじって「DNA アダクトーム解析」と命名した[6),7)]．DNA 付加体を質量分析により定量する場合，プリカーサーイオンとプロダクトイオンの質量差を 116 にするとうまく測定できることはすでに述べたが，プリカーサーイオンとプロダクトイオンの質量差を常に 116 に保ちながら，さまざまな質量について網羅的に解析することにより，未知の DNA 付加体を検出できる．現在われわれは感度の問題から，MRM モードを利用している．使用している LC/MS/MS (Waters-Micromass 社製，Quattro Pt) では，一度に最大 32 チャンネルの分析が可能なので，例えば同じサンプルを 15 回に分けて分析すれば，質量 266 から 629 の範囲について調べることができる (Fig.

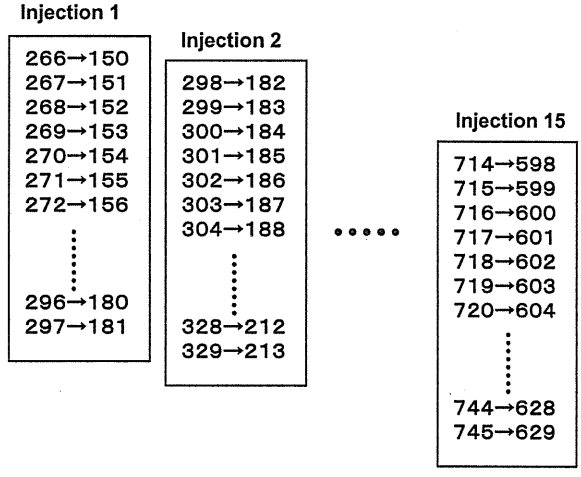

Fig. 3. An example of parameter-setting of precursor ion and product ion in DNA adductome analysis. Note that the difference of m/z between precursor ion and product ion is always 116.

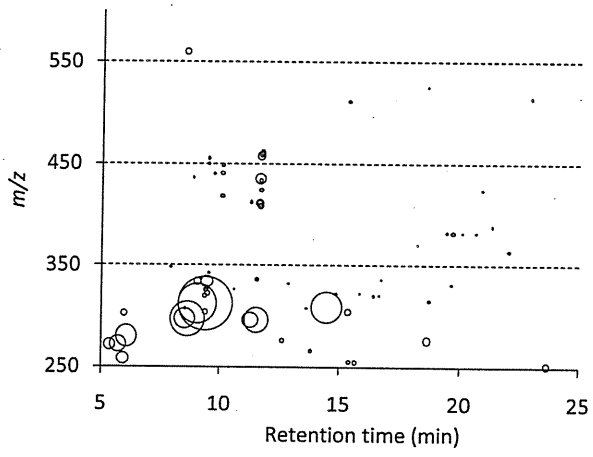

Fig. 4. An example of adductome map of human colon DNA. The horizontal axis is retention time of LC/MS/MS and the vertical axis is *m/z*. The size of the babble represent the area of detected peaks.

3). 今後技術革新により質量分析計の感度が上がればニュートラルロススキャンを使って，一度の分析で同じことができるようになるだろう．

Fig. 4 は，ヒトの大腸の DNA について，DNA アダクトーム解析した例である．出現したピーク（おそらく DNA 付加体由来）の面積をバブル図にプロットしている．質量分析では測定物質の構造によりイオン化の効率が異なるため，面積の大きなピークが必ずしも量が多い付加体に対応しているわけではないが，DNA アダクトーム解析により生体内に LC/MS/MS で検出可能な DNA 付加体が何種類ぐらいあり，その質量はどのくらいかという情報が得られる．われわれは，さまざまな DNA サンプルについてこの解析を進めており，重要な未知の DNA 付加体の構造決定を試みている．

6. おわりに

本稿では DNA 付加体の定量分析の分野では LC/MS/MS がすでに実用段階に入っており，主流になりつつあること，および，DNA アダクトームという方法を用いることにより，生物の臓器中に存在する未知の DNA 付加体の網羅的解析ができるということを紹介してきた．LC/MS/MS の技術革新に伴う感度や分解能の向上は目覚ましく，今後ますます簡便に，より網羅的に DNA 付加体が解析できるようになるだろう．これにより DNA 付加体の全容が明らかになれば，発がんや老化のメカニズム解明に役立つだろう．

謝　辞　本稿の発表の機会を与えていただいた，BMS コンファレンス実行委員の皆様に深く感謝いたします．なお，本稿で発表した内容は，NEDO (The New Energy and Industrial Technology Development Organization) 産業技術研究助成事業，日本学術振興会科学研究費補助金，厚生労働がん研究費により行った．

文　献

1) I. Terashima, N. Suzuki, and S. Shibutani, *Chem. Res. Toxicol.*, **15**, 305 (2002).
2) 松田知成，環境変異原研究，**26**, 199 (2004).
3) P. J. Brooks, *et al.*, *PLoS Medicine*, **6**, 258 (2009).
4) T. Matsuda, H. Yabushita, R. Kanaly, S. Shibutani, and A. Yokoyama, *Chem. Res. Toxicol.*, **19**, 1374 (2006).
5) H. Nagayoshi, *et al.*, *Mutat. Res.*, **673**, 74 (2009).
6) R. A. Kanaly, *et al.*, *Antioxidants & Redox Signaling*, **8**, 993 (2006).
7) R. Kanaly, S. Matsui, T. Hanaoka, and T. Matsuda, *Mutat. Res.*, **625**, 83 (2007).

Keywords: DNA adduct, LC/MS/MS, DNA adductome

Environmental and Molecular Mutagenesis 50:815–822 (2009)

Research Article

Dependence of DNA Double Strand Break Repair Pathways on Cell Cycle Phase in Human Lymphoblastoid Cells

Yoshio Takashima, Mayumi Sakuraba, Tomoko Koizumi, Hiroko Sakamoto, Makoto Hayashi, and Masamitsu Honma*

Division of Genetics and Mutagenesis, National Institute of Health Sciences, 1-18-1 Kamiyoga, Setagaya-ku, Tokyo 158-8501, Japan

DNA double-strand breaks (DSBs) are usually repaired by nonhomologous end-joining (NHEJ) or homologous recombination (HR). NHEJ is thought to be the predominant pathway operating in mammalian cells functioning in all phases of the cell cycle, while HR works in the late-S and G2 phases. However, relative contribution, competition, and dependence on cell cycle phases are not fully understood. We previously developed a system to trace the fate of DSBs in the human genome by introducing the homing endonuclease I-*Sce*I site into the thymidine kinase (*TK*) gene of human lymphoblastoid TK6 cells. Here, we use this system to investigate the relative contribution of HR and NHEJ for repairing I-*Sce*I-induced DSBs under various conditions. We used a novel transfection system, Amaxa™ nucleofector, which directly introduces the I-*Sce*I expression vector into cell nuclei. Approximately 65% of transfected cells expressed the I-*Sce*I enzyme and over 50% of the cells produced a single DSB in the genome. The relative contribution of NHEJ and HR for repairing the DSB was ~100:1 and did not change with transfection efficiency. Cotransfection with KU80-siRNA significantly diminished KU80 protein levels and decreased NHEJ activity, but did not increase HR. We also investigated HR and NHEJ in synchronized cells. The HR frequency was 2–3 times higher in late-S/G2 phases than in G1, whereas NHEJ was unaffected. Even in late-S/G2 phases, NHEJ remained elevated relative to HR. Therefore, NHEJ is the major pathway for repairing endonuclease-induced DSBs in mammalian cells even in late-S/G2 phase, and does not compete with HR. Environ. Mol. Mutagen. 50:815–822, 2009.

Key words: double strand breaks (DSBs); I-*Sce*I site; non-homologous end joining (NHEJ); homologous recombination (HR); human cells

INTRODUCTION

Chromosomal double-strand breaks (DSBs) can be caused by ionizing radiation, chemicals, or endogenous processes that include V(D)J recombination and meiotic exchange. If these lesions are not repaired or are misrepaired, they can result in genomic rearrangement or cell death. The repair of DSBs is therefore essential for the maintenance of genomic integrity [Olive, 1998; van Gent et al., 2001]. The two major pathways responsible for such repair are homologous recombination (HR) and nonhomologous end joining (NHEJ) [Haber, 2000; Jackson, 2002]. As HR repairs DSBs using the undamaged homologous sequence as a template, we hypothesize that HR would take place mainly in the late-S and G2 phases of the cell cycle, when sister chromatids are available as templates. NHEJ, in contrast, should operate in all cell cycle phases. Many studies examining the relative contribution of NHEJ and HR in the repair of ionizing radiation-induced DSBs, demonstrate that their contribution varies with cell cycle phase [Takata et al., 1998; Rothkamm et al., 2003]. Ionizing radiation, however, produces not only DSBs but also single-strand breaks, various kinds of base and sugar damage, DNA interstrand crosslinks, and DNA-protein crosslinks [Brenner and Ward, 1992].

"Yoshio Takashima is currently at Research Center for Radiation Emergency Medicine, National Institute of Radiological Sciences, 4-9-1 Anagawa, Inage-ku, Chiba-shi, 263-8555, Japan."

*Correspondence to: Masamitsu Honma, Division of Genetics and Mutagenesis, National Institute of Health Sciences, 1-18-1 Kamiyoga, Setagaya-ku, Tokyo 158-8501, Japan. E-mail: honma@nihs.go.jp

Received 25 November 2008; provisionally accepted 18 January 2009; and in final form 19 January 2009

DOI 10.1002/em.20481

Published online 28 April 2009 in Wiley InterScience (www.interscience.wiley.com).

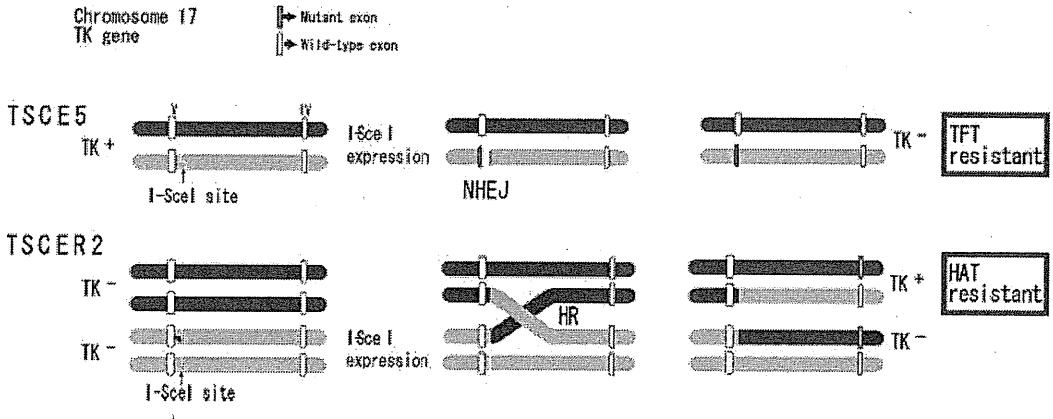

Fig. 1. Detection of NHEJ and HR in TSCE5 and TRSCR2 cells, respectively. Closed and shadowed bars represent mutant and wild-type alleles. In TSCE5, when a DSB at the I-*Sce*I site is repaired by NHEJ, a deletion results in exon 5, and TK-deficient mutants can be isolated in TFT medium. In TSCER2, when HR repairs the DSB, TK-proficient revertants are generated. The revertants can be selected in HAT medium.

Therefore, ionizing radiation-induced damage may not be ideal for the study of DSB repair. Recently, an understanding of DSB repair has emerged from systems that use the rare cutting restriction endonuclease from *Saccharomyces cerevisiae*, I-SceI [Johnson and Jasin, 2001]. Because the 18-bp recognition sequence of the I-*Sce*I gene is not present in most mammalian genomes and can be introduced by transfection, it is possible to generate site-specific DSBs in a mammalian chromosome or plasmid by expressing the I-SceI enzyme in genetically modified cells. This system was used to demonstrate that DSBs initiated HR and NHEJ of mammalian chromosomes. Most studies using this system, however, use artificial reporter substrates based on exogenous drug-resistance genes or a fluorescence gene, or are biased toward detecting specific deletion and recombination events [Sargent et al., 1997; Taghian and Nickoloff, 1997; Lin et al., 1999; Golding et al., 2004].

We previously developed a system to trace the fate of DSBs that occur in endogenous single-copy human genes [Honma et al., 2003, 2007]. Using gene-targeting, we introduced an I-*Sce*I site into the endogenous thymidine kinase (*TK*) gene of human lymphoblastoid TK6 cells, and developed cell lines that can detect NHEJ (TSCE5) and HR (TSCER2). TSCE5 is heterozygous (+/−) and TSCER2 is compound heterozygous (−/−) for the *TK* gene, and both have an I-*Sce*I site in intron 4. A DSB can be generated at the I-*Sce*I site by introducing I-SceI enzyme expression vector into the cells. NHEJ of the DSB results in TK-deficient mutants in TSCE5 cells, whereas HR between the alleles produces TK-proficient revertants in TSCER2 cells. The positive–negative drug selection assays for the TK phenotypes enable the distinction between NHEJ and HR events (Fig. 1). The assay system does not detect the genetic outcome of every NHEJ or HR event, because small deletion or small tract recombination that does not change the TK phenotype cannot be recovered. Furthermore, sister-chromatid recombination, which is also very important in HR, is also missed. Nonetheless, the system is very useful for understanding the role and mechanism of DSB repair in mammalian cells.

In the present study, we use the system described above to investigate the relative contribution of NHEJ and HR for repairing DSBs in TK6 cells. We also evaluate the dependence of both types of repair on cell cycle phases in synchronized cells. To understand the competition or cooperation between NHEJ and HR, we investigate repair activity in NHEJ knock-down cells generated by siRNA technology.

MATERIALS AND METHODS

Cell lines and Vectors

We used human lymphoblastoid cell lines TSCE5 and TSCER2, which are TK6 cells with an I-*Sce*I site inserted into the *TK* locus [Honma et al., 2003]. TSCE5 cells are heterozygous (*TK* +/−) for a point mutation in exon 4, and TSCER2 cells are compound heterozygous (*TK* −/−) for a point mutation in exons 4 and 5. NHEJ for a DSB occurring at the I-*Sce*I site results in TK-deficient mutants (*TK* −/−) in TSCE5 cells, while HR between the alleles produces TK-proficient revertants (TK +/−) in TSCER2 cells (Fig. 1). Cells were grown in RPMI 1640 medium (Gibco-BRL, Life technology, Grand Island, NY) supplemented with 10% heat-inactivated horse serum (JRH Biosciences, Lenexa, KS), 200 μg/ml sodium pyruvate, 100 U/ml penicillin, and 100 μg/ml streptomycin and maintained them at 10^5 to 10^6 cells/ml at 37°C in a 5% CO_2 atmosphere with 100% humidity.

The I-*Sce*I-expression vector, pCBASce, (kindly provided by Dr. Shunichi Takeda, Kyoto University) contains the coding sequences of the I-*Sce*I endonuclease from *Saccharomyces cerevisiae* under the control of the β-actin gene promoter [Fukushima et al., 2001]. We also constructed a pCBASce-off vector from pCBASce by inserting a 28-bp DNA fragment containing the 18-bp I-*Sce*I-restriction sequence between the 3′-end of its I-*Sce*I-nuclease coding sequence and a poly (A) site.

The expression of the I-SceI endonuclease of the pCBASce-off vector destroys the vector itself. Hence, its expression should be lost following transfection.

I-SceI Expression and Detection of NHEJ and HR

We electroporated ~5 × 10^6 cells using Amaxa™ nucleofector (Amaxa Biosystems, Gaithersburg, MD), program A-30, in solution V (provided by the supplier) with 50 μg/ml I-*SceI* expression vector, pCBASce or pCBASce-off. After 72 hr, cells were seeded into 96-well plates with trifluorothymidine (TFT) (for TK-mutants) or hypoxanthine, aminopterin, and thymidine (HAT) (for TK-revertants) medium. Drug resistant colonies were counted 2 weeks later.

Flow Cytometric and Microscopic Analysis with Immunofluorescence

We examined the post transfection kinetics of I-SceI expression using an anti-hemagglutinin A (HA) antibody [Guirouilh-Barbat et al., 2004] because the pCBASce vector coexpresses HA-tag together with I-SceI enzyme. Cells were fixed in 4% paraformaldehyde for 15 min at room temperature and permeabilized with 0.1% Triton X-100 (Sigma, St. Louis, MO) for 10 min. Immunofluorescence analysis was performed with an anti-HA antibody conjugated with Alexa Fluor 488 (Covance, Berkeley, CA), and transfection efficiency analyzed with an Epics XL flow cytometer (Beckman Coulter, Fullerton, CA) according to the manufacturer's recommendations.

Cells were also fixed with methanol on glass slides and immersed in PBS containing 0.5% Triton X100 for 30 min. To detect DSBs within individual cells, we conducted immunohistochemical analysis using gamma-H2AX antibody. The fixed cells were treated with a rabbit anti-phospho-gamma-H2AX antibody (Trevigen, Gaithersburg, MD), and then treated with a second antibody, goat Alexa Flour 488 anti-rabbit IgG (Invitrogen Japan KK, Tokyo, Japan).Cells were rinsed with PBS, stained with 4′,6-diamino-2-phenylindole dihydrochlorine (DAPI), and observed with a fluorescent microscope (Olympus, Tokyo, Japan).

siRNA and Western Blot Analysis

Cells were transfected with 50 nM KU80 small interfering RNA (siRNA; Santa Cruz Biotechnology, Santa Cruz, CA) using Amaxa™ nucleofector and Nucleofection Kit V. After 24-hr and 48-hr incubations, cell extracts were Western blotted using anti-KU86 (Santa Cruz Biotechnology) and anti-β-actin (Sigma) antibodies. Blots were exposed to horseradish peroxidase-labeled secondary antibodies (Amersham Pharmacia Biotech, Arlington Heights, IL), visualized using an enhanced chemiluminescence detection system, and quantified by densitometric scanning.

Cell Cycle Synchronization

A 2-step procedure was used to synchronize cells that included treatment with nocodazole (Sigma) followed by hydroxyurea (Sigma) because extended exposure to either chemical is genotoxic [Timson, 1975; Sun et al., 2005]. Cells were treated with 1 μM nocodazole for 12 hr followed by 2 mM hydroxyurea for 6 h to obtain a G1 rich cell population. Several hours later, following removal to a drug-free medium, the cell population shifted to the S/G2 phase. Cell cycle synchronization was established by flow cytometry. Cells were periodically harvested, washed in phosphate buffered saline (PBS), fixed in 70% cold ethanol, treated with 20 μg/ml RNase A (Wako Pure Chemical, Osaka, Japan), and stained with 10 μg/ml propidium iodide (Wako Pure Chemical). Approximately 10,000 cells per each sample were examined by EPICS-XL flow-cytometer (Beckman Coulter), and the data were quantitatively analyzed by MultiCycle AV software (Version. 4.0, Phoenix Flow Systems, San Diego, CA). A student's *t*-test was used to identify statistically significant differences in mutant frequencies.

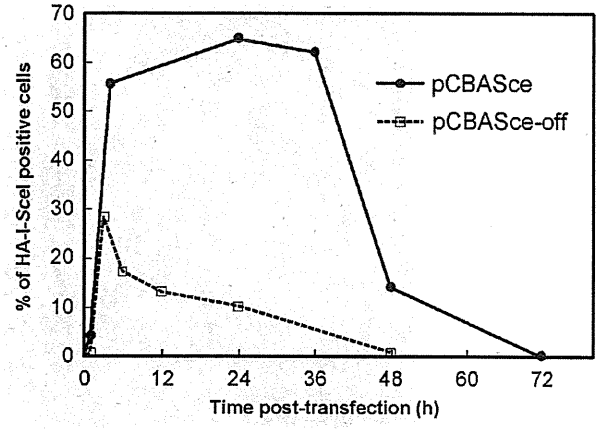

Fig. 2. Kinetics of I-*SceI* expression after transfection of pCBASce and pCBASce-off vectors. Detection of the anti-HA antibody tagged enzyme by flow cytometry.

RESULTS AND DISCUSSION

Expression of I-SceI and Generation of DSBs

The expression of the I-SceI enzyme in TSCE5 and TSCER2 cells generates a DSB in the *TK* gene. To introduce the expression vector into the cells, we used the Amaxa™ nucleofection system, which can directly transfer DNA into the nucleus at high efficiency [Honma et al., 2007]. We examined the kinetics of I-SceI expression by flow cytometry. The HA-tag attached to the I-SceI enzyme's amino terminus permits expression monitoring (Fig. 2). Expression was immediately apparent following introduction of pCBASce vector into TSCE5 cells. Twenty-four hours later, 65% of the cell population expressed the HA-tag. The expression continued to 48 hr, but not 72 hr. We also examined gamma-H2AX, a marker of DSBs [Fernandez-Capetillo et al., 2003; Nakamura et al., 2006]. Imunohistochemical analysis demonstrated that over 50% of the nucleofected cells showed a single DSB in their nuclei (Fig. 3). These results indicate that our I-SceI system with Amaxa™ nucleofection efficiently and specifically produced a DSB at the target site. The data also suggest that DSBs continue to occur up to at least 48 hr after nucleofection. Some DSBs may repeatedly occur and be repaired during that period, if an error-free pathway predominates [Honma et al., 2007].

We also developed a pCBASce-off vector based on pCBASce. This vector contains the 18 bp I-*SceI* restriction sequence between the 3′-end of I-*SceI*-nuclease coding sequence and the poly (A) site. The kinetics of

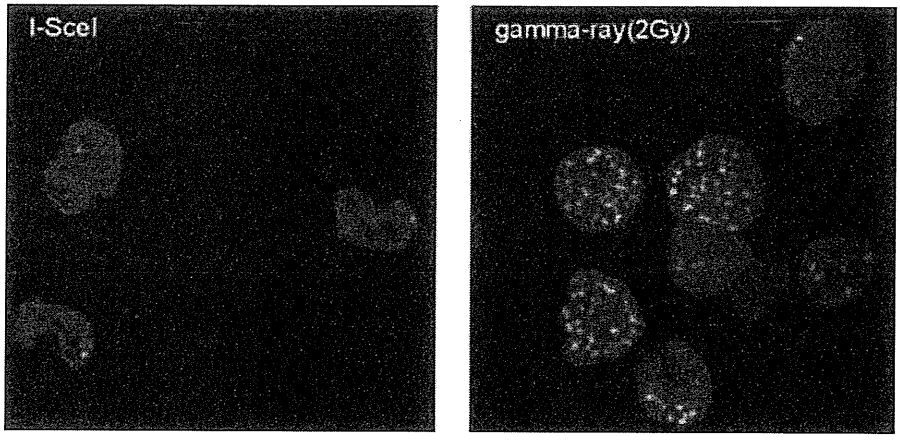

Fig. 3. Detection of DSBs by immunohistochemical analysis with gamma-H2AX antibody. Gamma-H2AX foci (green) in TSCE5 cells transfected with pCBASce vector (left) and cells irradiated with 2Gy gamma-ray (right). Nuclei were stained with DAPI. The transfection of pCBASce vector produced a single DSB in a TSCE5 cell at high efficiency.

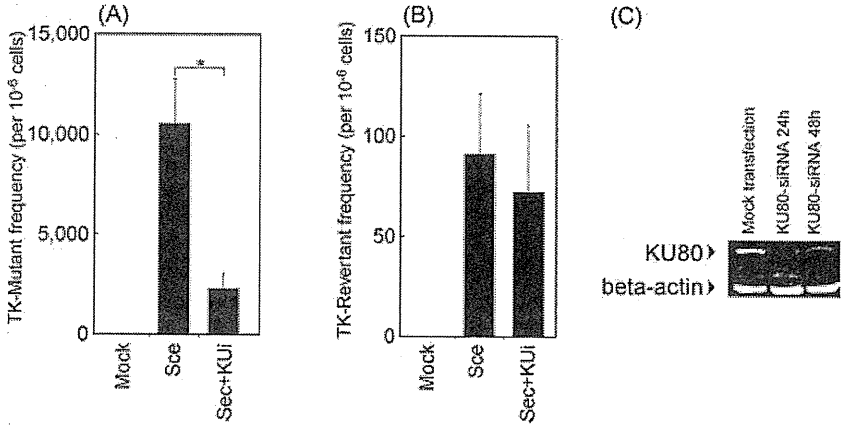

Fig. 4. Frequencies of TK-deficient mutants in TSCE5 (A) and TK-proficient revertants in TSCER2 (B). Mock-transfected control cells (Mock), cells transfected with the pCBASce vector (Sce), cells co-transfected with KU80 siRNA and the pCBASce vector (Sce+KU-i). The data are presented as the mean ± SD of 5 independent experiments; bars are SD. *$P < 0.05$. (C): Expression of KU80 protein. TSCE5 cells were transfected with KU80-siRNAs, and were conducted by Western blot analyses at 24 hr and 48 hr later after the transfection.

expression of the pCBASce-off vector is also shown in Figure 2. The expression of pCBASce-off vector reached a peak at 4 hr following transfection and immediately decreased. No expression was observed 48 hr later. This indicates that the pCBASce-off vector was destroyed by I-SceI-nuclease in the cells, and a DSB temporarily occurs in the *TK* gene. This may provide a more suitable model than DSBs caused by ionizing radiation, although the DSBs in the model do not correspond exactly with exogenous DSBs, and the DSB induction-efficiency is quite low. However, the model is useful to study cell-cycle dependent DNA repair and mutagenesis of DSBs.

NHEJ and HR for I-SceI-Induced DSBs in KU80-Competent and Knockdown Cells

Figures 4A and 4B show the frequency of the TK-deficient mutants in TSCE5 and TK-proficient revertants in TSCER2 cells. These mutants are the consequence of DSBs repaired by NHEJ and HR, respectively. The TK-deficient mutant frequency was 2.0×10^{-6} in the control TSCE5 cells. Introduction of the pCBASce vector elevated the frequency up to 1.1×10^{-2}, which was about 5,000 times higher than observed in control cells (Fig. 4A). The revertant frequency in TSCER2 also increased up to 0.9×10^{-4} following introduction of pCBASce

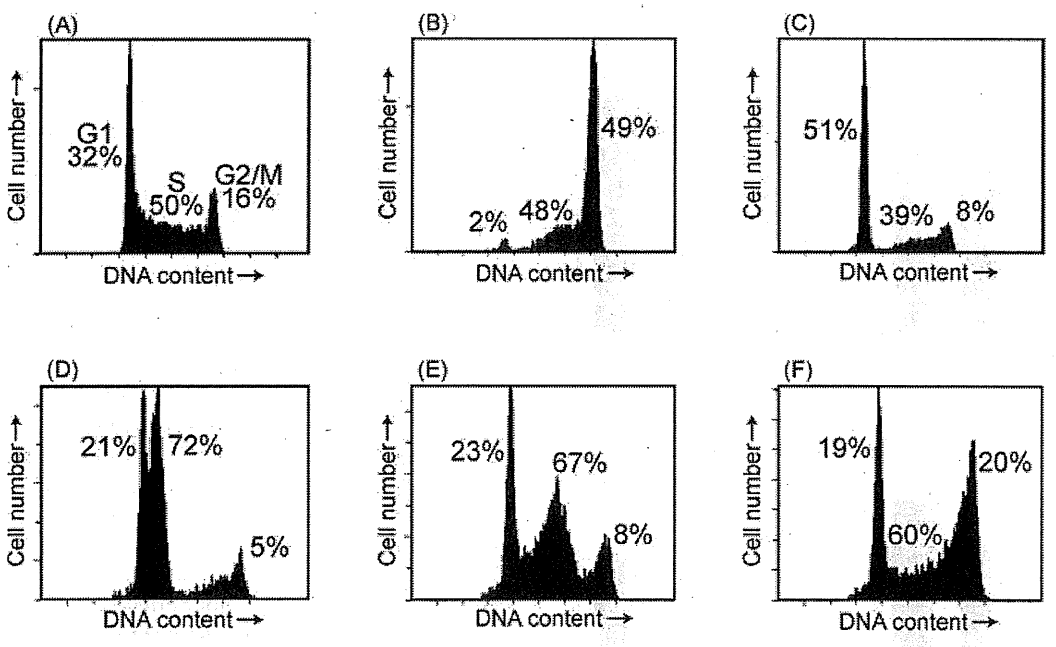

Fig. 5. DNA histograms for synchronization of cell cycle. Nonsynchronized cells (**A**) were arrested in the M phase with nocodazole (1 μM) for 12 hr, and (**B**) released into the media containing hydroxyurea (1 mM). After 6 hr incubation, the cells were arrested at the G1/S boundary (**C**), and released into a drug-free medium. The cells synchronously progressed through the cell cycle after being released from the hydroxyurea block (**D–F**). Cell cycle synchronization was confirmed by flow cytometry.

vector (Fig. 4B). These results suggest that the DSBs induced by the restriction enzyme are efficiently repaired by both NHEJ and HR. However, the relative contribution of NHEJ and HR was ~100:1, similar to our previous findings [Honma et al., 2007].

When TSCE5 and TSCER2 cells were transfected with the pCBASce-off vector, the TK-deficient mutant frequency was 1.6×10^{-3} in the TSCE5 cells, and the TK-revertant frequency was 1.3×10^{-5} in the TSCER2 cells. The lower frequency of mutants and revertants resulting from pCBASce-off relative to pCBASce is likely due to the low efficiency of expression of pCBASce-off (Fig. 2). However, the relative contribution of NHEJ and HR was not influenced.

Western blot analysis demonstrated that siRNA-mediated knockdown of KU80 proteins in the cells resulted in 94% and 75% reduction of KU protein at 24 hr and 48 hr after the transfection, respectively (Fig. 4C). TSCE5 cells that were cotransfected with the pCBASce vector and KU80 siRNA exhibited significantly lower NHEJ frequency (0.22×10^{-2}) than when the pCBASce vector alone was transfected (1.1×10^{-2}) (Fig. 4A). Conversely, HR frequency induced by DSBs in TSCER2 was not altered by KU80 knockdown (Fig. 4B). This suggests that NHEJ and HR do not simply compete for I-SceI induced DSBs [Delacote et al., 2002].

KU80 plays a major role in the NHEJ pathway for DSB repair in mammalian cells. It is believed that KU80 and KU70 bind to the DNA end, then recruit DNA-PKcs and stabilize their binding [Smith and Jackson, 1999; Lieber et al., 2003; Downs and Jackson, 2004]. A decrease in the TK-deficient mutant frequency following cotransfection with KU80 siRNA indicates that the TK-deficient mutants induced I-*Sce*I expression by NHEJ. However, NHEJ still predominantly repairs DSBs in the KU80-knockdown cells, which may reflect the activity of the remaining NHEJ by leaky KU80 protein or the presence of an alternative end-joining pathway [Iliakis et al., 2004; Lieber, 2008]. Schulte-Uentrop et al. suggested different genetic requirements for repairing I-SceI-induced DSBs because KU80 knock-out mouse cells did not lose end-joining activity for I-SceI-induced DSBs [Schulte-Uentrop et al., 2008]. Wu et al. proposed a backup NHEJ pathway (B-NHEJ) utilizing Ligase III and PARP-1 as an alternative to the classical DNA-PKcs dependent pathway (D-NHEJ) [Wu et al., 2008]. It was demonstrated that the efficiency of end-joining for restriction enzyme induced-DSBs was significantly suppressed in KU80 knock-out cells treated with PARP-1 inhibitors [Wang et al., 2006].

Contribution of NHEJ and HR in Repairing DSBs in Different Phases of the Cell Cycle

Cell cycles were synchronized using nocodasol (1 μM) and hydroxyurea (2 mM). Nonsynchronized cells (Fig. 5A) treated with nocodazole for 12 hr were arrested in M

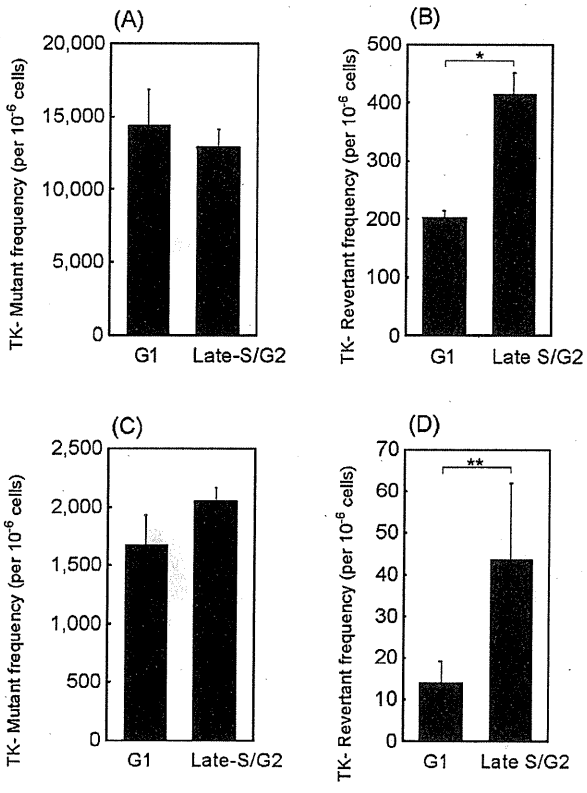

Fig. 6. Frequencies of TK-deficient mutants in synchronized TSCE5 cells (**A, C**) and of the TK-proficient revertants in synchronized TSCER2 cells. (A, C). The synchronized cells were transfected with pCBASce vector (A, **B**) and with pCBASce-off vector (C, **D**). The data are presented as the mean ± SD of three independent experiments; bars are SD. $*P < 0.05$, $**P < 0.1$.

phase (Fig. 5B) and released into the media containing hydroxylurea. After 6 hr incubation in hydroxyurea, cells were arrested at the G1/S boundary (Fig. 5C). The cells synchronously progressed through the cell cycle after being released from the hydroxyurea block (Figs. 5D–5F). Because I-SceI expression began 3 hr post transfection (Fig. 2), we transfected pCBASce vector into the cells at the M/G1 boundary (1 hr after release from the nocodazole block), and in early-S phase (1 hr after release from the hydroxyurea block) to efficiently generate DSBs at the G1 phase and the late-S/G2 phase, respectively. The cell populations at 3 hr following the transfection were as expected as shown in Figures 5D (G1) and 5E (late-S/G2).

The NHEJ frequency in the TSCE5 cells was 1.4×10^{-2} in the G1 phase and 1.3×10^{-2} in the late-S/G2 phase (Fig. 6A). In the TSCER2 cells, the HR frequency was 2.0×10^{-4} in the G1 phase and 4.1×10^{-4} in the late-S/G2 phase (Fig. 6B). Treatment with nocodazole and hydroxyurea did not affect colony-forming efficiency (data not shown). The HR frequency was twofold higher in late-S/G2 cells than in G1 cells, whereas the frequency of NHEJ was not dependent on cell-cycle phase. We also transfected the pCBASce-off vector into the synchronized cells (Figs. 6C and 6D). Because the pCBASce-off vector is only briefly expressed following transfection, analysis of cell cycle dependence should be clear. Although no difference was observed for NHEJ frequencies between G1 (1.7×10^{-3}) and late-S/G2 (2.0×10^{-3}) phases (Fig. 6C), the HR frequency in the late-S/G2 cells (4.3×10^{-5}) was threefold higher than in the G1 cells (1.4×10^{-5}) (Fig. 6D). These results suggest that HR function is dependent on cell cycle, and is more active in the late-S/G2 phase.

The contribution of NHEJ and HR to the repair of DSBs in mammalian cells varies with the systems used to detect them [Rothkamm et al., 2003; Mao et al., 2008a]. In the present work, we demonstrated that NHEJ is equally functional in all cell cycle phases, whereas HR operates 2–3 times more efficiently in late-S/G2 than in G1. Because we could not completely synchronize the cell population, and could not perfectly introduce a DSB into the specific cell population even by using pCBASce-off vector, quantitative analysis for cell-cycle dependence of DSB repair is difficult. Saleh-Gohari and Helleday demonstrated that by using synchronized human cells containing a stably integrated copy of a recombination reporter gene, the frequency of HR repair of DSBs was 24-fold higher in S-phase cells than in G1/G0 cells [Saleh-Gohari and Helleday, 2004]. However, they did not examine the relative contributions of NHEJ and HR throughout the cell cycle phases. Recently, Mao et al. measured the efficiency of NHEJ and HR at different cell cycle stages in hTERT-immortalized diploid human fibroblast cells. They showed that the overall efficiency of NHEJ was higher than HR at all cell cycle stages, although HR works more efficiently in the S-phase [Mao et al., 2008b].

The conclusions of the present work support those described above. We demonstrate that NHEJ is the predominant mechanism for DSB repair even in late-S/G2 phase. Our systems, however, are unable to detect sister-chromatid recombination (SCR), which must be an important recombination event during late-S/G2 phase [Helleday, 2003]. Because SCR is an error-free pathway and does not leave any genetic change in principle, it is impossible to quantitatively measure SCR at the molecular level. Most systems for studying HR are designed to detect unusual SCR events that occur in artificial recombination substrates [Bertrand et al., 1997; Boehden et al., 2003; Richardson et al., 2004]. Because the I-SceI enzyme during the late-S/G2 phase cleaves both sister-chromatids, SCR may not occur in our system. Occasionally, if one of two sister-chromatids are broken, SCR may arise. If SCR predominantly works during late-S/G2 phase, NHEJ frequency must be suppressed. The lack of

change in NHEJ frequency across all phases of the cell cycle implies that NHEJ is the major DSB repair pathway and does not compete with HR. HR may be involved in a more prolonged attempt to repair persistent DNA lesions [Delacote et al., 2002; Frank-Vaillant and Marcand, 2002; Kim et al., 2005]. While I-SceI induced a single DSB, ionizing radiation and chemicals induce many different types of DNA damage [Nikjoo et al., 1997]. DSBs also endogenously arise by replication fork stalling or collapse during S phase [Delacote and Lopez, 2008; Llorente et al., 2008]. These lesions are thought to be repaired by strand invasion into a homologous duplex DNA followed by replication or HR [Llorente et al., 2008]. Therefore, the relative contribution of NHEJ and HR to DSB repair varies with the character of the lesion and the number of DSBs induced in the genome.

REFERENCES

Bertrand P, Rouillard D, Boulet A, Levalois C, Soussi T, Lopez BS. 1997. Increase of spontaneous intrachromosomal homologous recombination in mammalian cells expressing a mutant p53 protein. Oncogene 14:1117–1122.

Boehden GS, Akyuz N, Roemer K, Wiesmuller L. 2003. p53 mutated in the transactivation domain retains regulatory functions in homology-directed double-strand break repair. Oncogene 22:4111–4117.

Brenner DJ, Ward JF. 1992. Constraints on energy deposition and target size of multiply damaged sites associated with DNA double-strand breaks. Int J Radiat Biol 61:737–748.

Delacote F, Lopez BS. 2008. Importance of the cell cycle phase for the choice of the appropriate DSB repair pathway, for genome stability maintenance: The trans-S double-strand break repair model. Cell Cycle 7:33–38.

Delacote F, Han M, Stamato TD, Jasin M, Lopez BS. 2002. An xrcc4 defect or Wortmannin stimulates homologous recombination specifically induced by double-strand breaks in mammalian cells. Nucleic Acids Res 30:3454–3463.

Downs JA, Jackson SP. 2004. A means to a DNA end: The many roles of Ku. Nat Rev Mol Cell Biol 5:367–378.

Fernandez-Capetillo O, Celeste A, Nussenzweig A. 2003. Focusing on foci: H2AX and the recruitment of DNA-damage response factors. Cell Cycle 2:426–427.

Frank-Vaillant M, Marcand S. 2002. Transient stability of DNA ends allows nonhomologous end joining to precede homologous recombination. Mol Cell 10:1189–1199.

Fukushima T, Takata M, Morrison C, Araki R, Fujimori A, Abe M, Tatsumi K, Jasin M, Dhar PK, Sonoda E, Chiba T, Takeda S. 2001. Genetic analysis of the DNA-dependent protein kinase reveals an inhibitory role of Ku in late S-G2 phase DNA double-strand break repair. J Biol Chem 276:44413–44418.

Golding SE, Rosenberg E, Khalil A, McEwen A, Holmes M, Neill S, Povirk LF, Valerie K. 2004. Double strand break repair by homologous recombination is regulated by cell cycle-independent signaling via ATM in human glioma cells. J Biol Chem 279: 15402–15410.

Guirouilh-Barbat J, Huck S, Bertrand P, Pirzio L, Desmaze C, Sabatier L, Lopez BS. 2004. Impact of the KU80 pathway on NHEJ-induced genome rearrangements in mammalian cells. Mol Cell 14:611–623.

Haber JE. 2000. Partners and pathwaysrepairing a double-strand break. Trends Genet 16:259–264.

Helleday T. 2003. Pathways for mitotic homologous recombination in mammalian cells. Mutat Res 532:103–115.

Honma M, Izumi M, Sakuraba M, Tadokoro S, Sakamoto H, Wang W, Yatagai F, Hayashi M. 2003. Deletion, rearrangement, and gene conversion; genetic consequences of chromosomal double-strand breaks in human cells. Environ Mol Mutagen 42:288–298.

Honma M, Sakuraba M, Koizumi T, Takashima Y, Sakamoto H, Hayashi M. 2007. Non-homologous end-joining for repairing I-SceI-induced DNA double strand breaks in human cells. DNA Repair (Amst) 6:781–788.

Iliakis G, Wang H, Perrault AR, Boecker W, Rosidi B, Windhofer F, Wu W, Guan J, Terzoudi G, Pantelias G. 2004. Mechanisms of DNA double strand break repair and chromosome aberration formation. Cytogenet Genome Res 104:14–20.

Jackson SP. 2002. Sensing and repairing DNA double-strand breaks. Carcinogenesis 23:687–696.

Johnson RD, Jasin M. 2001. Double-strand-break-induced homologous recombination in mammalian cells. Biochem Soc Trans 29:196–201.

Kim JS, Krasieva TB, Kurumizaka H, Chen DJ, Taylor AM, Yokomori K. 2005. Independent and sequential recruitment of NHEJ and HR factors to DNA damage sites in mammalian cells. J Cell Biol 170:341–347.

Lieber MR. 2008. The mechanism of human nonhomologous DNA end joining. J Biol Chem 283:1–5.

Lieber MR, Ma Y, Pannicke U, Schwarz K. 2003. Mechanism and regulation of human non-homologous DNA end-joining. Nat Rev Mol Cell Biol 4:712–720.

Lin Y, Lukacsovich T, Waldman AS. 1999. Multiple pathways for repair of DNA double-strand breaks in mammalian chromosomes. Mol Cell Biol 19:8353–8360.

Llorente B, Smith CE, Symington LS. 2008. Break-induced replication: What is it and what is it for? Cell Cycle 7:859–864.

Mao Z, Bozzella M, Seluanov A, Gorbunova V. 2008a. Comparison of nonhomologous end joining and homologous recombination in human cells. DNA Repair (Amst) 7:1765–1771.

Mao Z, Bozzella M, Seluanov A, Gorbunova V. 2008b. DNA repair by nonhomologous end joining and homologous recombination during cell cycle in human cells. Cell Cycle 7:2902–2906.

Nakamura A, Sedelnikova OA, Redon C, Pilch DR, Sinogeeva NI, Shroff R, Lichten M, Bonner WM. 2006. Techniques for gamma-H2AX detection. Methods Enzymol 409:236–250.

Nikjoo H, O'Neill P, Goodhead DT, Terrissol M. 1997. Computational modelling of low-energy electron-induced DNA damage by early physical and chemical events. Int J Radiat Biol 71:467–483.

Olive PL. 1998. The role of DNA single- and double-strand breaks in cell killing by ionizing radiation. Radiat Res 150:S42–S51.

Richardson C, Stark JM, Ommundsen M, Jasin M. 2004. Rad51 overexpression promotes alternative double-strand break repair pathways and genome instability. Oncogene 23:546–553.

Rothkamm K, Kruger I, Thompson LH, Lobrich M. 2003. Pathways of DNA double-strand break repair during the mammalian cell cycle. Mol Cell Biol 23:5706–5715.

Saleh-Gohari N, Helleday T. 2004. Conservative homologous recombination preferentially repairs DNA double-strand breaks in the S phase of the cell cycle in human cells. Nucleic Acids Res 32: 3683–3688.

Sargent RG, Brenneman MA, Wilson JH. 1997. Repair of site-specific double-strand breaks in a mammalian chromosome by homologous and illegitimate recombination. Mol Cell Biol 17:267–277.

Schulte-Uentrop L, El Awady RA, Schliecker L, Willers H, Dahm-Daphi J. 2008. Distinct roles of XRCC4 and Ku80 in non-homologous end-joining of endonuclease- and ionizing radiation-induced DNA double-strand breaks. Nucleic Acids Res 36:2561–2569.

Smith GC, Jackson SP. 1999. The DNA-dependent protein kinase. Genes Dev 13:916–934.

Sun F, Betzendahl I, Pacchierotti F, Ranaldi R, Smitz J, Cortvrindt R, Eichenlaub-Ritter U. 2005. Aneuploidy in mouse metaphase II oocytes exposed in vivo and in vitro in preantral follicle culture to nocodazole. Mutagen 20:65–75.

Taghian DG, Nickoloff JA. 1997. Chromosomal double-strand breaks induce gene conversion at high frequency in mammalian cells. Mol Cell Biol 17:6386–6393.

Takata M, Sasaki MS, Sonoda E, Morrison C, Hashimoto M, Utsumi H, Yamaguchi-Iwai Y, Shinohara A, Takeda S. 1998. Homologous recombination and non-homologous end-joining pathways of DNA double-strand break repair have overlapping roles in the maintenance of chromosomal integrity in vertebrate cells. EMBO J 17:5497–5508.

Timson J. 1975. Hydroxyurea. Mutat Res 32:115–132.

van Gent DC, Hoeijmakers JH, Kanaar R. 2001. Chromosomal stability and the DNA double-stranded break connection. Nat Rev Genet 2:196–206.

Wang M, Wu W, Wu W, Rosidi B, Zhang L, Wang H, Iliakis G. 2006. PARP-1 and Ku compete for repair of DNA double strand breaks by distinct NHEJ pathways. Nucleic Acids Res 34:6170–6182.

Wu W, Wang M, Wu W, Singh SK, Mussfeldt T, Iliakis G. 2008. Repair of radiation induced DNA double strand breaks by backup NHEJ is enhanced in G2. DNA Repair (Amst) 7:329–338.

Accepted by—
C. Menck

TOXICOLOGICAL SCIENCES 109(1), 96–105 (2009)
doi:10.1093/toxsci/kfp037
Advance Access publication February 23, 2009

The Mouse Lymphoma Assay Detects Recombination, Deletion, and Aneuploidy

Jianyong Wang,*,[1] Jeffrey R. Sawyer,† Ling Chen,*,‡ Tao Chen,* Masamitsu Honma,§ Nan Mei,* and Martha M. Moore*,[2]

*Division of Genetic and Reproductive Toxicology, National Center for Toxicological Research/ Food and Drug Administration, 3900 NCTR Road, Jefferson, AR 72079; †Cytogenetics Laboratory, Department of Pathology, University of Arkansas for Medical Sciences, Little Rock, AR 72205; ‡College of Life Science and Technology, Shanghai Jiao Tong University, Shanghai, China; and §Division of Genetics and Mutagenesis, National Institute of Health Sciences, Tokyo 158-8501, Japan

Received October 31, 2008; accepted January 29, 2009

The mouse lymphoma assay (MLA) uses the thymidine kinase (*Tk*) gene of the L5178Y/$Tk^{+/-}$-3.7.2C mouse lymphoma cell line as a reporter gene to evaluate the mutagenicity of chemical and physical agents. The MLA is recommended by both the United States Food and Drug Administration and the United States Environmental Protection Agency as the preferred *in vitro* mammalian cell mutation assay for genetic toxicology screening because it detects a wide range of genetic alterations, including both point mutations and chromosomal mutations. However, the specific types of chromosomal mutations that can be detected by the MLA need further clarification. For this purpose, three chemicals, including two clastogens and an aneugen (3′-azido-3′-deoxythymidine, mitomycin C, and taxol), were used to induce *Tk* mutants. Loss of heterozygosity (LOH) analysis was used to select mutants that could be informative as to whether they resulted from deletion, mitotic recombination, or aneuploidy. A combination of additional methods, G-banding analysis, chromosome painting, and a real-time PCR method to detect the copy number (CN) of the *Tk* gene was then used to provide a detailed analysis. LOH involving at least 25% of chromosome 11, a normal karyotype, and a *Tk* CN of 2 would indicate that the mutant resulted from recombination, whereas LOH combined with a karyotypically visible deletion of chromosome 11 and a *Tk* CN of 1 would indicate a deletion. Aneuploidy was confirmed using G-banding combined with chromosome painting analysis for mutants showing LOH at every microsatellite marker on chromosome 11. From this analysis, it is clear that mouse lymphoma *Tk* mutants can result from recombination, deletion, and aneuploidy.

Key Words: **mouse lymphoma assay; mutation type; loss of heterozygosity; cytogenetics; copy number; 3′-azido-3′-deoxythymidine; mitomycin C; taxol; thymidine kinase.**

The mouse lymphoma assay (MLA), using the thymidine kinase (*Tk*) gene of the L5178Y/$Tk^{+/-}$-3.7.2C mouse lymphoma cell line as a reporter gene of mutation, is preferred by a number of international regulatory agencies, including the United States Food and Drug Administration and the United States Environmental Protection Agency, as the *in vitro* mammalian mutation assay in the genetic toxicology screening battery. The decision to prefer the MLA was based on previous research demonstrating that the assay detects most of the mutational events known to be associated with the etiology of cancer and other human diseases, including point mutations and a number of different types of chromosomal mutations (Applegate *et al.*, Blazak *et al.*, 1989; Chen *et al.*, 2002; Clive *et al.*, 1990; 1990; Honma *et al.*, 2001; Hozier *et al.*, 1981, 1992; Liechty *et al.*, 1998; Moore *et al.*, 1985; Zhang *et al.*, 1996).

It is important to determine the various mutation types that can be detected by this assay, so that MLA data can be properly interpreted. Since the development of this assay, quite a number of studies have been conducted to understand the types of mutations that can be detected by the MLA. Several cytogenetic studies have been conducted to analyze *Tk* mutants induced by various mutagens (Blazak *et al.*, 1986, 1989; Hozier *et al.*, 1981; Moore *et al.*, 1985; Zhang *et al.*, 1996). It is clear that many small colony (SC) mutants have recognizable chromosome rearrangements involving chromosome 11, which contains the *Tk* gene. The Tk^- and Tk^+ chromosomes can be distinguished by a centromeric heteromorphism: the Tk^+ chromosome has a bigger centromere (Hozier *et al.*, 1982; Sawyer *et al.*, 1985). This finding greatly helps the cytogenetic characterization of chromosome aberrations in *Tk* mutants. However, without the help of molecular genetics, small chromosome changes cannot be detected using cytogenetic methods alone; mitotic recombination cannot be identified because the karyotype of the mutant would be normal. Applegate *et al.* (1990) identified a *Nco I* restriction fragment length polymorphism that distinguishes the Tk^+ and Tk^- alleles. Several studies using Southern blot analysis to determine the status of the Tk^+ allele were subsequently conducted (Applegate *et al.*, 1990; Clive *et al.*, 1990). The

[1] Present address: Office of New Drugs, Center for Drug Evaluation and Research, Food and Drug Administration, HFD-540, 10903 New Hampshire Avenue, Silver Spring, MD 20993.

[2] To whom correspondence should be addressed at Division of Genetic and Reproductive Toxicology, National Center for Toxicological Research/FDA, 3900 NCTR Rd, Jefferson, AR 72079. Fax: 870-543-7393. E-mail: martha.moore@fda.hhs.gov.

presence of the Tk^+ allele suggests an intragenic mutation, while the loss of the Tk^+ allele indicates a chromosome mutation. Most large colony (LC) mutants induced by point mutagens, such as ethyl methanesulfonate, retain the Tk^+ allele; while most SC mutants induced by clastogens, such as bleomycin, lose the Tk^+ allele. An allele-specific PCR technique was developed to identify the presence or absence of the Tk^+ allele. Furthermore, based on microsatellite polymorphisms, the loss of heterozygosity (LOH) pattern of the entire chromosome 11 can be investigated (Liechty *et al.*, 1994, 1996, 1998). This labor-saving approach allows many mutants to be analyzed; however, without the detection of *Tk* gene copy number (CN), one cannot distinguish between a deletion and a recombination event. Southern blot analysis can be used to detect *Tk* gene CN (Applegate *et al.*, 1990), but it is resource intensive, requires a relatively large amount of DNA, and the measurement is not precise (Joseph *et al.*, 1993). Therefore, we developed a real-time PCR method to detect the CN of the *Tk* gene (Wang *et al.*, 2007). By combining LOH analysis of chromosome 11 and cytogenetic analysis, we were able to distinguish between deletion and recombination events.

Another important issue for the MLA is whether the assay can detect aneuploidy. Aneuploidy plays a significant role in many adverse human health conditions, including spontaneous abortions, birth defects, and cancer (Aardema *et al.*, 1998; Duesberg *et al.*, 1999; Oshimura and Barrett, 1986; Sen, 2000). Aneugens can interact with the spindle apparatus or impair its function, thereby inducing aneuploidy due to nondisjunction mechanisms. Several aneugens are carcinogens (Cimino *et al.*, 1986; Oshimura and Barrett, 1986). Although the MLA has been shown to detect aneugens, its ability to adequately detect aneuploidy is unclear. Applegate *et al.* (1990) reported that at least some *Tk* mutants show aneuploidy. Honma *et al.* (2001) evaluated two aneugens, colchicine, and vinblastine, using the MLA. The two chemicals did not induce a significant mutant frequency (MF) increase after the regular 3-h treatment. Although they did show positive responses after the long-term (24 h) treatment, the increase of MF was not high. Therefore, many of the mutants that were isolated and analyzed from the chemical-treated cultures would be spontaneous rather than induced mutants.

Overall, the specific types of chromosomal mutations that are detected by the MLA need further clarification. In this study, *Tk* mutants from cultures treated with different chemicals, including two clastogens and an aneugen (3′-azido-3′-deoxythymidine [AZT], mitomycin C and taxol), were used. A combined strategy of both molecular genetic and cytogenetic methods was used to analyze the mutants. LOH analysis of chromosome 11 was conducted first, and then the *Tk* mutants showing LOH involving a large portion of chromosome 11 were selected for further cytogenetic analysis and *Tk* CN detection. It should be noted that it was not our intent to provide a complete analysis of the types of mutational events induced by these three chemicals; rather, we used these chemicals to give us mutants for our analysis that would be expected to include deletions, mitotic recombination, and aneuploidy.

MATERIALS AND METHODS

Cell culture. The L5178Y/$Tk^{+/-}$ -3.7.2C mouse lymphoma cells were cultured in suspension using Fischer's medium for leukemic cells of mice (Quality Biologicals, Gaithersburg, MD) supplemented with 10% heat-inactivated horse serum, 200 μg/ml sodium pyruvate, 100 unit/ml penicillin, 100 μg/ml streptomycin, and 0.05% (vol/vol) pluronic F68 (Invitrogen, Carlsbad, CA). The cultures were incubated at 37°C in an atmosphere of 5% CO_2 and saturated humidity and maintained in logarithmic growth.

Tk mutant induction. *Tk* mutants isolated from AZT-treated and taxol-treated cultures were from previous studies using the microwell version of the assay (Moore *et al.*, 2005; Wang *et al.*, 2007). For the induction of *Tk* mutants using mitomycin C (obtained from Sigma, St Louis, MO), the protocol for the microwell version of the mouse lymphoma assay described by Chen and Moore (2004) was followed. Briefly, cells were centrifuged and resuspended at a concentration of 0.2×10^6 cells/ml in 50 ml of medium in 75-cm^2 polystyrene flasks. Mitomycin C dissolved in dimethyl sulfoxide (DMSO) was added from a stock solution to the cell cultures. Additional DMSO was added to give a final volume of 100 μl. The flasks were incubated for 4 h, and then the cells were centrifuged, washed twice, and resuspended in fresh medium. The cells were transferred to new 75-cm^2 flasks and cultured for 2 days for mutant expression with cell counts and cell density adjustment made after 1 day. Then the cells were cloned in 96-well plates in medium containing 3 μg/ml trifluorothymidine (TFT) for selection and medium without TFT for the measurement of cloning efficiency. After 12 days, the 96-well plates were evaluated by eye using a Quebec dark field colony counter to determine the presence or absence of colonies in each well and to enumerate the number of small and LC mutants. Total MF, SC MF, and LC MF were determined, and the relative total growth values that measures cytotoxicity were calculated according to the published protocol (Chen and Moore, 2004). Mutant colonies were randomly selected and isolated from the cultures treated with the highest test dose of AZT (1 mg/ml), mitomycin C (0.4 μg/ml), or taxol (1 μg/ml), respectively.

DNA extraction. The isolated mutant colonies were cultured in fresh medium for several days to obtain sufficient cells for subsequent analysis. Genomic DNA was extracted from 3×10^6 cells of each *Tk* mutant clone using the Qiagen DNeasy tissue kit (Valencia, CA) and stored at − 20°C.

Tk gene LOH analysis. *Tk* gene LOH analysis was conducted using the allele-specific PCR described by Liechty *et al.* (1996), with some modifications (Wang *et al.*, 2007). Basically, the microsatellite locus *D11Agl2* that resides in the *Tk* gene was amplified using a touchdown PCR method. The PCR was performed in 96-well plates using a PCR System 9700 (Applied Biosystems, Foster City, CA). The reaction products were separated by 2% agarose gel electrophoresis, stained with 1 μg/ml ethidium bromide, and visualized with a UV light box.

Chromosome 11 LOH analysis. In addition to microsatellite marker *D11Agl2*, eight other microsatellite loci on mouse chromosome 11 (*D11Mit 42, 59, 36, 29, 22, 20, 19*, and *74*) were used (Wang *et al.*, 2007). The nine microsatellite loci are almost evenly distributed along the length of the chromosome (with locations at 78.0, 72.0, 58.5, 47.6, 40.0, 25.0, 20.0, 13.0, and 0.0cM, respectively). LOH analysis was performed at each microsatellite locus using allele-specific PCR as previously described (Wang *et al.*, 2007). The PCR products were separated and visualized as above.

Tk gene dosage analysis. For those mutants showing LOH involving a large portion of chromosome 11 (at least including microsatellite markers *D11Agl2* and *D11Mit 42*), *Tk* gene CN was evaluated using the real-time PCR $2^{-\Delta\Delta Ct}$ method described previously (Wang *et al.*, 2007). Briefly, a fragment of the *Tk* gene and a fragment of an unrelated gene (*H-2K*) on chromosome

17 were amplified simultaneously. The *H-2K* gene fragment was used as an endogenous reference for PCR relative quantitation.

According to the criteria set by Honma *et al.* (2001), the CN of *Tk* mutants was classified as <1.2, 1.2–1.8, and >1.8, which sets the ranges for the hemizygous, mosaic, and homozygous states of the *Tk* gene, respectively.

G-banding analysis. For the mutants showing LOH involving a large portion of chromosome 11 (at least including microsatellite markers *D11Agl2* and *D11Mit 42*), G-banding analysis was performed to examine the alteration of chromosome 11. The protocol established by Sawyer *et al.* (1985) was followed with some revision. Briefly, a 12-ml cell culture (approximately 8–10 $\times$ 10^6 cells) was centrifuged at 200 $\times$ g for 10 min. The supernatant was discarded, and the cell pellet was resuspended with gentle agitation in a hypotonic solution (10 ml 75mM KCl). Then 120 µl of 10 µg/ml colchicine (Sigma) was added. The cell suspension was then incubated at 37°C for 20 min. Five drops of fixative (5:2, methanol:acetic acid) were added at the end of incubation with gentle agitation to avoid cell clumping. Then the cells were centrifuged, and the supernatant was discarded leaving approximately 0.5 ml of solution over the pellet. The pellet was then gently agitated, and 10 ml of fixative was added. After gentle mixing, the cell suspension was incubated at room temperature for 20 min. The cell suspension was centrifuged, and the fixative was changed twice to eliminate cell debris and to ensure good spreading and staining of chromosomes. The cell pellet was resuspended in about 1 ml fixative to make the slides. For karyotypic analysis, cells were dropped onto precleaned glass slides (soaked in 95% ethanol overnight) and air dried. Trypsin treatment before Giemsa staining was used to sharpen bands and increase contrast. At least 10 cells were examined per clone.

Chromosome painting analysis. Chromosome 11 painting analysis was performed as described by Zhang *et al.* (1996) with some modification. Briefly, colchicine was added to a 12-ml cell culture (approximately 8–10 $\times$ 10^6 cells) at a final concentration of 0.5 µg/ml. Cells were incubated for 1 h at 37°C in an atmosphere of 5% CO_2 and saturated humidity. Then the cell culture was centrifuged at 200 $\times$ g for 10 min and resuspended in hypotonic solution (75mM KCl), followed by incubation in a water bath at 37°C for 20 min. After that, five drops of fixative (3:1, methanol:acetic acid) were added with gentle agitation. The rest of the cell fixation was accomplished using the procedure described in the G-banding analysis section above.

A whole-chromosome painting probe specific for mouse chromosome 11 labeled with biotin was purchased from Cambio (Cambridge, UK). The chromosome painting procedure described in the manufacturer's instructions was followed. Briefly, chromosomal DNA on slides was denatured with 2× sodium chloride-sodium citrate buffer (SSC)-70% formamide solution (1× SSC is 0.15M NaCl + 0.015M sodium citrate) at 70°C for 2 min followed by dehydration through an ethanol series (70%, 85%, and 100%). Probes were added to the metaphase preparations. After overnight hybridization at 37°C, the slides were washed three times with 2× SSC-50% formamide solution and three times with 2× SSC at 45°C. The slides were then incubated with fluorescent avidin-DCS (Vector Laboratories, Burlingame, CA) solution at 37°C for 30 min and washed with 2× SSC containing 0.1% Tween 20. The slides were then incubated with biotinylated goat anti-avidin DCS (Vector Laboratories) at 37°C for 30 min followed by a second fluorescent avidin-DCS treatment. The slides were washed, counterstained with propidium iodide solution, and mounted. At least 10 metaphases from each slide were examined with fluorescence microscopy.

RESULTS

The *Tk* MFs for the AZT-, mitomycin C–, and taxol-treated cultures used for mutant analysis are shown in Table 1. The complete MF data for AZT can be found in Wang *et al.* (2007), for taxol in Moore *et al.*, (2005), and for mitomycin C in Figure 1. At the highest dose tested, all three chemicals induced high *Tk* MFs (4.8-, 16.6-, and 7.3-fold over the concurrent negative control for AZT, mitomycin C, and taxol, respectively). This indicated that most of the analyzed *Tk* mutants were chemical-induced mutants rather than spontaneous background mutants.

TABLE 1
***Tk* Gene MFs in Mouse Lymphoma Cells Treated with AZT, Mitomycin C, and Taxol (at the Highest dose Tested)**

			Tk MF ($\times$ 10^{-6})	
Chemical	Concentration	SC[a] (%)	Control	Treated culture
AZT[b]	1 mg/ml	65%	84	407
Mitomycin C	0.4 µg/ml	44%	56	928
Taxol[c]	1 µg/ml	41%	50	366

[a]SC mutants, as a percent of all *Tk* mutant colonies obtained.
[b]Data from Wang *et al.* (2007).
[c]Data from Moore et al. (2005).

For our detailed analysis to determine if mutants can result from deletion, mitotic recombination, and aneuploidy, we needed mutants with large chromosomal alterations. Therefore, a number of mutants were first screened using nine microsatellite markers spanning chromosome 11. Mutants showing partial chromosome 11 LOH including at least microsatellite markers *Agl2* and *Mit42* were selected for further analysis using G-banding. In addition, *Tk* gene CN of these mutants was evaluated. Chromosome painting analysis was performed for some of the mutants showing LOH at every chromosome 11 microsatellite marker.

Fifteen mutants from the 1-mg/ml AZT–treated culture (Wang *et al.*, 2007) showing LOH including at least microsatellite markers *Agl2* and *Mit42* were analyzed using G-banding analysis. Nineteen mutants from the 0.4-µg/ml mitomycin C–treated culture were analyzed using chromosome 11 LOH analysis; then four mutants showing partial chromosome 11 LOH were analyzed using *Tk* gene dosage analysis and G-banding analysis, and two mutants showing LOH at

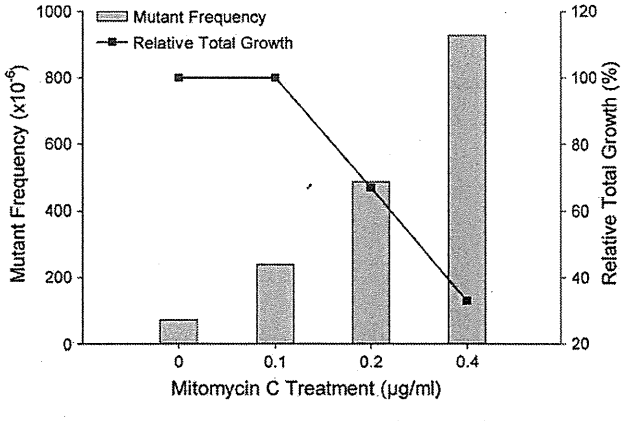

FIG. 1. *Tk* gene MFs and relative total growth values of mouse lymphoma cells treated with mitomycin C.

TABLE 2
The Number of Mutants that were Analyzed Using G-banding Analysis or Chromosome Painting Analysis

Treatment	LOH pattern	Number of mutants analyzed using G-banding analysis	Number of mutants analyzed using chromosome painting analysis
1 mg/ml AZT	Partial LOH including at least microsatellite markers *Agl2* and *Mit42*	15	
0.4 μg/ml mitomycin C	Partial LOH including at least microsatellite markers *Agl2* and *Mit42*	4	
	Complete LOH		2
1 μg/ml taxol	Complete LOH		7

every microsatellite marker on chromosome 11 were analyzed using chromosome painting analysis. Twenty mutants from the 1-μg/ml taxol–treated culture were isolated for chromosome 11 LOH analysis, and seven mutants showing LOH at every microsatellite marker on chromosome 11 were analyzed using chromosome painting analysis. The number of mutants that were analyzed using the combined strategy is summarized in Table 2.

The results of the G-banding analysis can be classified as normal chromosome 11, visible deletion, or complex chromosome alterations. The number of chromosome 11 revealed by the chromosome painting analysis can be classified as one (indicating chromosome loss), two (indicating chromosome duplication after loss), or more than two (including either aneuploidy or polyploidy). The numbers of metaphase spreads showing different numbers of chromosome 11 as revealed by chromosome painting are shown in Table 3. The combined results of the chromosome 11 LOH analysis, *Tk* CN detection, and G-banding/chromosome painting analysis are shown in Table 4.

TABLE 3
The Number of Metaphase Spreads Showing Different Numbers of Chromosome 11 in the *Tk* Mutants Isolated from Mitomycin C– or Taxol-Treated Cultures as Revealed by Chromosome Painting

	Number of chromosome 11				
Mutant[a]	1	2	3	4	>4
ML7	1	9	0	0	0
MS3	3	4	2	1	0
TL2	2	8	0	0	0
TL4	0	9	0	1	0
TL8	3	7	0	0	0
TS2	1	7	0	1	1
TS4	0	8	1	1	0
TS6	0	2	5	0	3
TS7	2	8	0	0	0

[a]The first letter of the mutant name indicates the chemical exposure (M, mitomycin C; T, taxol); the second letter indicates colony size of the mutant (L, large; S, small). All the mutants showed LOH at every microsatellite marker on chromosome 11. Ten metaphase spreads were counted for each *Tk* mutant.

In total, 28 mutants showing partial or complete chromosome 11 LOH were analyzed using this combined strategy. Among them, nine mutants (A1B4, A1B5, A2D4, A3C2, A5B3, A6A2, ML4, ML10, and MS6) retained a normal karyotype, while at least three microsatellite markers showed LOH. With a *Tk* CN of 2, the mutation type of these mutants can be identified as recombination. A representative metaphase cell is shown in Figure 2. Five mutants (A1C6, A3A4, A5C2, A5D6, and A6C2) were identified to be deletions. They all have partial chromosome 11 LOH patterns, one copy of the *Tk* gene, and chromosome 11 showing visible deletions or deletions combined with translocation (representative metaphase cell shown in Fig. 2). Five mutants (A5C6, A5D2, A7B5, A7C1, and MS8) showed complex chromosome alterations. They all have partial chromosome 11 LOH patterns, with more than one copy of the *Tk* gene. G-banding analysis showed that the Tk^- chromosome appears to be normal, while the Tk^+ chromosome is abnormally long (Fig. 3). It is speculated that this complex alteration was the result of multiple events: deletion, duplication (aneuploidy), and translocation. First, the Tk^+ chromosome was partially deleted, which resulted in the LOH pattern; then the Tk^- chromosome was duplicated and translocations occurred. The duplicated Tk^- chromosome was translocated directly to the damaged Tk^+ chromosome or other chromosomes. Mutants A5D2 and MS8 have *Tk* CNs between 1 and 2, indicating that they are mosaic mutants. They may be a mixture of cells with duplicated Tk^- chromosome after the partial deletion of the Tk^+ chromosome or the Tk^- chromosome was not duplicated. For those mutants that showed complete LOH of chromosome 11 (ML7, MS3, TL2, TL4, TL8, TS2, TS4, TS6, and TS7), chromosome painting analysis indicated that they were all mosaic mutants, and overall the major mechanism appears to be the Tk^- chromosome duplication after the loss of the Tk^+ chromosome. Representative photos for chromosome loss and chromosome duplication after loss are shown in Figure 4.

DISCUSSION

A complete evaluation of genetic toxicology data includes an analysis of the mode of action by which the test chemical induced mutation (Dearfield and Moore, 2005). Because there are a number of genotoxicity tests and different tests detect different types of genotoxic damage, they may give a mixture of both positive and negative results. Therefore, it is important to identify the types of mutations detected by the different assays in order to evaluate the data properly.

As mentioned before, it has been established that the MLA can detect both point mutations and chromosomal mutations

TABLE 4

Combined Results of the LOH Analysis, *Tk* Gene CN Detection, and G-Banding/Chromosome Painting Analysis for the *Tk* (Mutants Isolated from AZT-, Mitomycin C–, or Taxol-Treated Cultures

		LOH pattern[c]										
		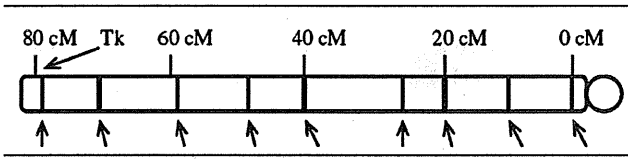										
		80 cM Tk		60 cM		40 cM		20 cM		0 cM		
Mutants[a]	L/S[b]	*Agl2*	*42*	*59*	*36*	*29*	*22*	*20*	*19*	*74*	*Tk* CN[d]	G-banding/chromosome painting[e]
A1B4	L	○	○	○	○	○	●	●	●	●	>1.8	Recombination
A1B5	L	○	○	○	○	●	●	●	●	●	>1.8	Recombination
A1C6	L	○	○	●	●	●	●	●	●	●	<1.2	Deletion
A2D4	L	○	○	○	●	●	●	●	●	●	>1.8	Recombination
A3A4	S	○	○	●	●	●	●	●	●	●	<1.2	Deletion
A3C2	S	○	○	○	○	○	●	●	●	●	>1.8	Recombination
A5B3	S	○	○	○	○	○	●	●	●	●	>1.8	Recombination
A5C2	S	○	○	●	●	●	●	●	●	●	<1.2	Deletion
A5C6	S	○	○	○	●	●	●	●	●	●	>1.8	Deletion with aneuploidy
A5D2	S	○	○	○	●	●	●	●	●	●	1.2–1.8	Deletion with/without aneuploidy
A5D6	S	○	○	○	○	●	●	●	●	●	<1.2	Deletion with translocation
A6A2	S	○	○	○	●	●	●	●	●	●	>1.8	Recombination
A6C2	S	○	○	○	●	●	●	●	●	●	<1.2	Deletion
A7B5	S	○	○	○	●	●	●	●	●	●	>1.8	Deletion with aneuploidy
A7C1	S	○	○	○	●	●	●	●	●	●	>1.8	Deletion with aneuploidy
ML4	L	○	○	○	○	●	●	●	●	●	>1.8	Recombination
ML10	L	○	○	○	●	●	●	●	●	●	>1.8	Recombination
MS6	S	○	○	○	●	●	●	●	●	●	>1.8	Recombination
MS8	S	○	○	●	●	●	●	●	●	●	1.2–1.8	Deletion with/without aneuploidy
ML7	L	○	○	○	○	○	○	○	○	○	NA[f]	Chromosome loss/duplication
MS3	S	○	○	○	○	○	○	○	○	○	NA	Chromosome loss/duplication
TL2	L	○	○	○	○	○	○	○	○	○	NA	Chromosome loss/duplication
TL4	L	○	○	○	○	○	○	○	○	○	NA	Chromosome duplication
TL8	L	○	○	○	○	○	○	○	○	○	NA	Chromosome loss/duplication
TS2	S	○	○	○	○	○	○	○	○	○	NA	Chromosome loss/duplication
TS4	S	○	○	○	○	○	○	○	○	○	NA	Chromosome duplication
TS6	S	○	○	○	○	○	○	○	○	○	NA	Chromosome duplication
TS7	S	○	○	○	○	○	○	○	○	○	NA	Chromosome loss/duplication

●, retain heterozygosity; ○, LOH.

[a]The first letter of the mutant name indicates the chemical exposure. A, AZT; M, mitomycin C; T, taxol. For mutants from AZT-treated culture, LOH analysis and *Tk* gene CN detection was done in a previous study (Wang *et al.*, 2007).

[b]L, large colony mutant; S, small colony mutant.

[c]*D11Agl2, D11Mit 42, 59, 36, 29, 22, 20, 19,* and *74* are nine microsatellite markers that are almost evenly distributed along the length of chromosome 11.

[d]The *Tk* gene CN analysis was performed for mutants showing microsatellite LOH for at least markers *Agl2* and *Mit 42* but also retaining microsatellite heterozygosity for at least marker *Mit 74* (partial LOH of chromosome 11).

[e]G-banding analysis was performed for the mutants showing LOH at least at microsatellite markers *Agl2* and *Mit 42* but also retaining heterozygosity at least at microsatellite marker *Mit 74* (partial LOH of chromosome 11). Chromosome painting analysis was performed for the mutants showing LOH at every microsatellite marker on chromosome 11 (complete LOH of chromosome 11).

[f]Not analyzed.

(Applegate *et al.*, 1990; Chen *et al.*, 2002; Honma *et al.*, 2001; Hozier *et al.*, 1981; Liechty *et al.*, 1998; Moore *et al.*, 1985). A large experimental trial including 45 labs (Honma *et al.*, 1999) suggested that the MLA and the *in vitro* chromosome aberration test were basically "equivalent" as to their ability to give positive responses for clastogens. It is important to recognize that the MLA detects small-scale alterations that are too small to be detected by cytogenetic assays. In addition, the MLA detects recombination, which may lead to recessive mutations and plays an important role in the deactivation of

tumor suppressor genes during tumorigenesis. Recombination events are not detected by cytogenetic assays. Liechty *et al.* (1998) speculated that the MLA is able to detect recombination because of the autosomal location and the heterozygous status of the *Tk* gene. There is also evidence that the MLA can detect aneuploidy. It is especially important for regulatory purposes to collect more evidence demonstrating that the MLA is capable of detecting aneuploidy and recombination.

For our analysis, we needed mutants that were the result of deletion, mitotic recombination, or aneuploidy. For this purpose, we used three chemicals (AZT, mitomycin C, and taxol) to induce *Tk* mutants. AZT is a thymidine analogue that is clastogenic (Wang *et al.*, 2007). Mitomycin C is a potent clastogen, and it induces mutations in the *Tk* gene (Davies *et al.*, 1993; Dobrovolsky *et al.*, 2002). Taxol can impair cell spindles and induce aneuploidy (Ikui *et al.*, 2005; Mailhes *et al.*, 1999; Schiff and Horwitz, 1980).

As mentioned earlier, Honma *et al.* (2001) performed an analysis of *Tk* mutants using two aneugens, colchicine and vinblastine. The increase in MF was not very high, even after a 24-h treatment (3.6- and 2.3-fold over the control, for colchicine and vinblastine, respectively), so the mutants isolated and analyzed from these chemically treated cultures would include a large number of spontaneous mutants. In the present study, the MFs were much higher (4.8- to 16.6-fold over the control), indicating that many to most of the analyzed mutants were induced by the test chemicals.

Early cytogenetic studies of MLA *Tk* mutants showed that many SC mutants have recognizable chromosome aberrations involving the chromosome 11 that carries the Tk^+ allele. At that time, the chromosome aberrations identified in *Tk* mutants were primarily translocations (Blazak *et al.*, 1986; Hozier *et al.*, 1981; Moore *et al.*, 1985). Later, Southern blot analysis and an allele-specific PCR technique were used to determine the status of the *Tk* allele (Applegate *et al.*, 1990; Liechty *et al.*, 1994, 1996). Most of the SC mutants (both spontaneous and from treated cultures) and a large fraction of LC mutants (depending upon the mutagen) showed the loss of the Tk^+ allele, which indicates that the MLA is able to detect LOH, the most common mutational mechanism in human cancer.

Liechty *et al.* (1998) analyzed a large number of spontaneous *Tk* mutants using LOH analysis as well as chromosome painting. Their analysis provided evidence to support the hypothesis that the MLA detects recombination. However, the mutants they analyzed were all spontaneous

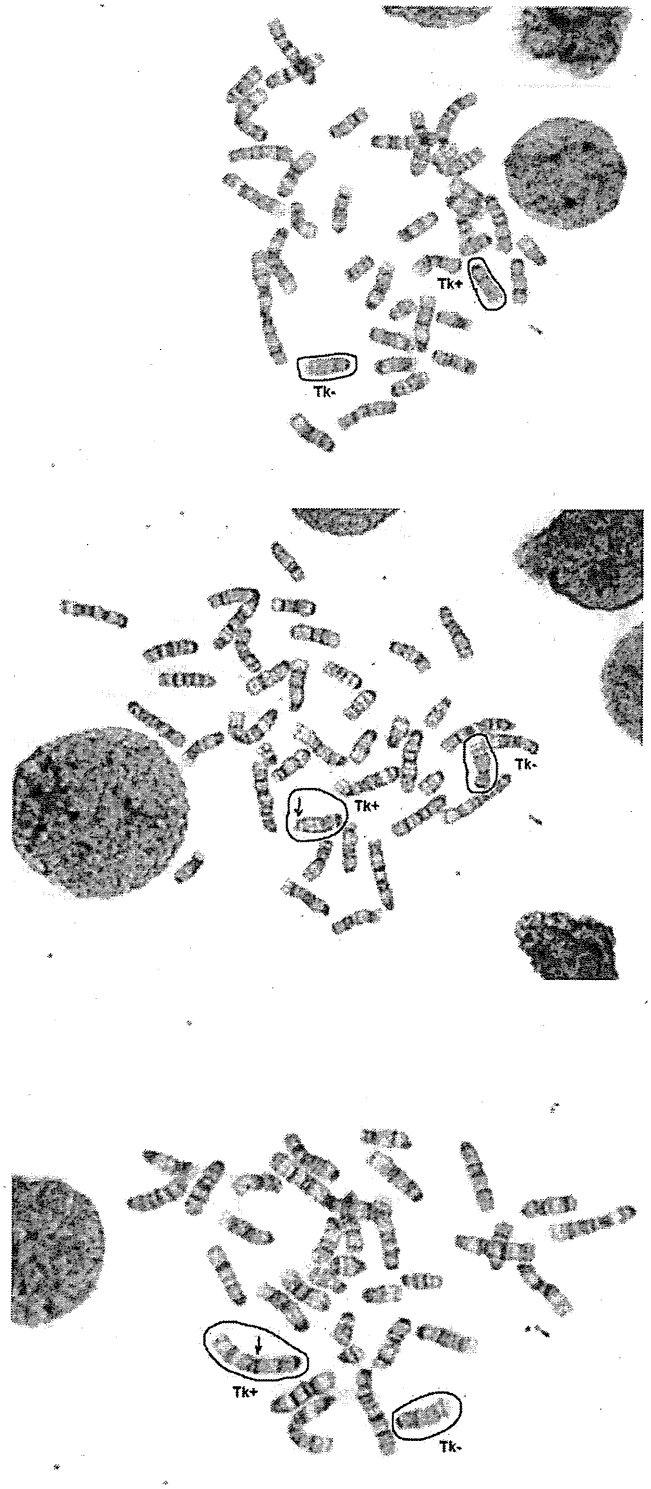

FIG. 2. G-banding analysis of mouse lymphoma *Tk* mutants A3C2, A6C2, and A5D6 that were isolated from a culture treated with 1 mg/ml AZT. The circled chromosomes are chromosome 11. The analysis of mutant A3C2 (top photo) shows a normal metaphase: two chromosome 11 with normal length and banding patterns (Tk^+ chromosome is on the right). The analysis of mutant A6C2 (middle photo) shows a visible deletion of the Tk^+ chromosome (left, indicated by an arrow). The Tk^- chromosome (right) has a normal banding pattern. The analysis of mutant A5D6 (bottom photo) shows a visible deletion of the distal Tk^+ chromosome resulting from an unbalanced translocation (translocation site indicated by an arrow). The Tk^- chromosome (right) has a normal banding pattern. Note that the Tk^+ chromosome has a bigger centromere than the Tk^- chromosome. This centromeric heteromorphism can be used to distinguish between the Tk^+ and Tk^- chromosomes.

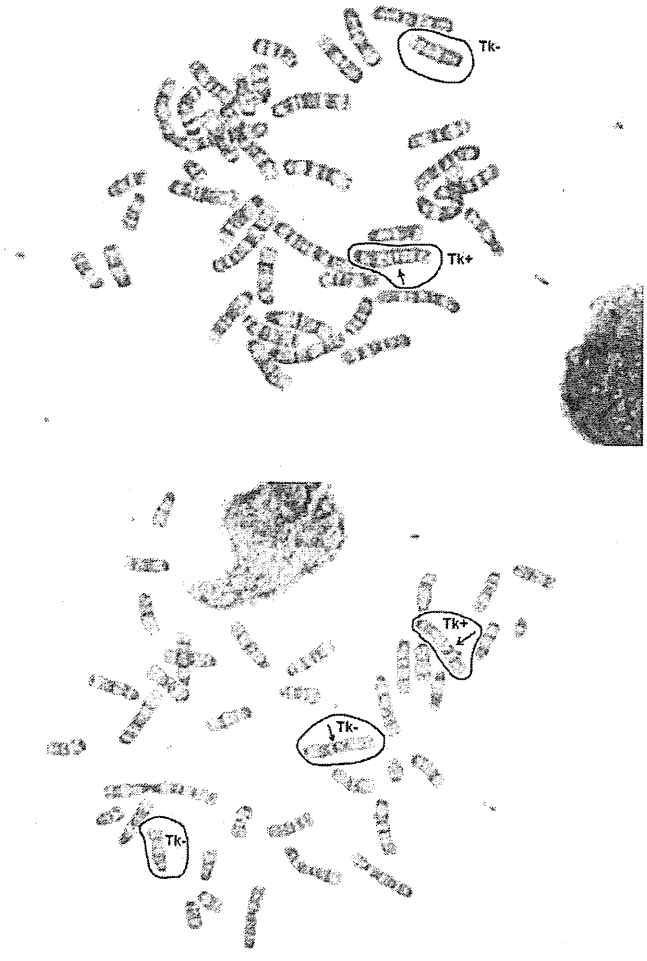

FIG. 3. G-banding analysis of mouse lymphoma *Tk* mutants MS8 (isolated from a cell culture treated with 0.4 μg/ml mitomycin C) and mutant A5D2 (isolated from a cell culture treated with 1 mg/ml AZT). Their metaphase cells display complex chromosome alterations. The circled chromosomes are chromosome 11. The Tk^+ chromosome has a bigger centromere than the Tk^- chromosome. This centromeric heteromorphism can be used to distinguish between the Tk^+ and Tk^- chromosomes. In the top photo for mutant MS8, the Tk^- chromosome (top) shows a normal banding pattern, while the Tk^+ chromosome (bottom) is abnormally long. It is formed by two chromosome 11 joined together (translocation site indicated by an arrow). In the bottom photo for mutant A5D2, two Tk^- chromosomes were identified: one (left) shows a normal banding pattern; the other (middle) is translocated to another chromosome (translocation site indicated by an arrow). The Tk^+ chromosome (right) was partially deleted by an unbalanced translocation (translocation site indicated by an arrow).

FIG. 4. Chromosome painting analysis of mouse lymphoma *Tk* mutants TL8 and TL2 that were isolated from a culture treated with 1 μg/ml taxol. The chromosome 11 probe is labeled with red fluorescence. The top photo for mutant TL8 shows only one chromosome 11 (chromosome loss). The bottom photo for mutant TL2 shows two chromosome 11 (chromosome duplication after loss).

mutants. In addition, although chromosome painting is relatively easy to perform and analyze, it is not as informative as conventional G-banding analysis. In their study, four mutants showed interesting chromosome alterations: two chromosome 11 with different lengths. Without G-banding analysis, those aberrations could not be identified. Previously we analyzed a mutant isolated from a bleomycin-treated culture (mutant 950, Clark *et al.*, 2004) and chromosome painting showed a similar result: two chromosome 11 with different lengths, with a partial LOH pattern. This was first interpreted as a deletion. However, further analysis using G-banding revealed

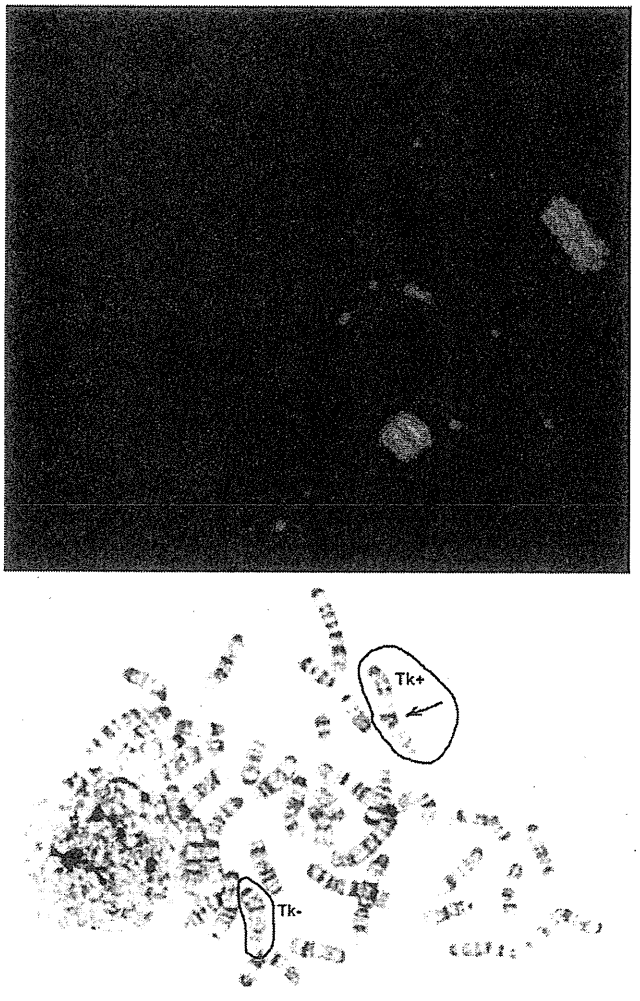

FIG. 5. Chromosome painting and G-banding analysis of mouse lymphoma *Tk* mutant 950 isolated from a bleomycin-treated culture (Clark *et al.*, 2004). The chromosome 11 probe is labeled with red fluorescence. Chromosome painting (top photo) shows two chromosome 11 of different length. The G-banding analysis (bottom photo) shows complex chromosome alterations. The circled chromosomes are chromosome 11. The Tk^- chromosome (left) shows a normal banding pattern, while the Tk^+ chromosome (right) is abnormally long. It is formed by two chromosome 11 joined together (translocation site indicated by an arrow). Note that the Tk^+ chromosome has a bigger centromere than the Tk^- chromosome. This centromeric heteromorphism can be used to distinguish between the Tk^+ and Tk^- chromosomes.

that the "longer" chromosome 11 was actually formed by two (or two parts of) chromosome 11 in an unbalanced translocation, while the "shorter" chromosome 11 was actually a normal Tk^- chromosome (Fig. 5). Therefore, in this study we used a combination of all the different analysis methods to identify the mutation types. Interestingly, five mutants (four from the AZT treatment and one from mitomycin C) were found to have alterations similar to mutant 950: deletion with aneuploidy. The proportion of this specific aberration in the mutants we analyzed is very high: 5 of the 19 analyzed were partial chromosome 11 LOH mutants. The underlying mechanism for this event is unclear. We speculate that the Tk^- chromosome duplication is some type of compensation for the deletion of the Tk^+ chromosome, resulting in partial trisomy (aneuploidy). This unique aberration may be related to the clastogenicity of the chemical: AZT, mitomycin C, and bleomycin are all clastogens.

Although chromosome loss is the primary mutation mechanism whereby aneugens induce Tk^--deficient mutants, few cells were found to be monosomic for chromosome 11 in this study. We analyzed nine mutants showing complete chromosome 11 LOH. The majority were mosaic with most having chromosome duplication after loss. This probably occurs because duplication of the Tk^- chromosome is a repair/compensation mechanism after the loss of the Tk^+ chromosome. Cells containing two Tk^- chromosomes would be expected to have a growth advantage over cells containing only one Tk^- chromosome, thereby becoming the predominant cell type in the culture (Honma *et al.*, 2001).

The results clearly demonstrate that MLA *Tk* mutants can result from recombination, deletion, and aneuploidy. The ability to detect recombination is a particular advantage of the MLA. Recombination is an important pathway for repairing DNA double-strand breaks, and it is essential for cellular survival in mammals (Helleday, 2003). It cannot be detected by assays using hemizygous reporter genes, such as *Hprt*. The ability to detect large deletions is another advantage of the MLA. This may be due to the *Trp53* status of the L5178Y/$Tk^{+/-}$ mouse lymphoma cell line. In this cell line, both alleles of the *Trp53* gene have point mutations, one of which likely results in no protein production (the point mutation produces a stop codon) and the other results in the production of a mutant Trp53 (Clark *et al.*, 1998; Storer *et al.*, 1997). Large-scale damage may be incompatible with the survival of Trp53-sufficient cells; these cells will undergo apoptosis under the surveillance of Trp53 (Honma *et al.*, 2000). The Trp53 status may also play a critical role in the ability of the MLA to detect aneuploidy (Honma *et al.*, 2001). In mammalian cells, Trp53 is involved in the maintenance of diploidy by participating in a mitotic checkpoint and the regulation of centrosome duplication (Cross *et al.*, 1995; Honma *et al.*, 2001; Tarapore and Fukasawa, 2000).

It should be emphasized that while this analysis indicates that the MLA can detect newly induced deletions, mitotic recombination, and aneuploidy, it does not provide insight into the relative proportion of the various types of mutational events or the efficiency with which these events are detected. While we have combined several powerful techniques to elucidate the mutations, all these techniques are very "blunt" tools. The nine LOH markers were distributed across chromosome 11, but from the perspective of potentially mutable sites, only a tiny fraction of the chromosome could be evaluated. Furthermore, our strategy of combining the G-banding analysis with the LOH analysis to distinguish between deletion and mitotic recombination required that the breakpoints be located so that at least approximately 25%

of the chromosome would be deleted (and readily visible by banded karyotype) if the mutant were a deletion rather than resulting from mitotic recombination.

To understand the mechanism for the induction of every mutant, and ultimately to fully understand the fundamental differences between the small and LC *Tk* mutants, the analysis must be conducted in a way that can interrogate a much larger portion of chromosome 11. We are currently initiating a research project to utilize comparative genomic hybridization microarray technology in combination with our current tools.

Our present study clearly demonstrates that the MLA can, in fact, detect deletion, recombination, and aneuploidy and provides new evidence for the utility of the MLA in a mechanistically based genotoxicity hazard identification battery. Depending upon the question that is being addressed and the importance of understanding the mutations induced by a particular chemical, our strategy of combining cytogenetic and molecular analysis of mutants can be used to provide more than a simple mutagenic/nonmutagenic hazard assessment.

FUNDING

Supported in part by an appointment (J.W.) to the Research Participation Program at the National Center for Toxicological Research administered by the Oak Ridge Institute of Science and Education (Oak Ridge, TN) through an interagency agreement between the U.S. Department of Energy and the U.S. Food and Drug Administration

ACKNOWLEDGMENTS

Disclaimer: The findings and conclusions in this report are those of the authors and do not necessarily represent the views of the U.S. Food and Drug Administration.

REFERENCES

Aardema, M. J., Albertini, S., Arni, P., Henderson, L. M., Kirsch-Volders, M., Mackay, J. M., Sarrif, A. M., Stringer, D. A., and Taalman, R. D. F. (1998). Aneuploidy: A report of an ECETOC task force. *Mutat. Res.* **410,** 3–79.

Applegate, M. L., Moore, M. M., Broder, C. B., Burrell, A., Juhn, G., Kasweck, K. L., Lin, P. F., Wadhams, A., and Hozier, J. C. (1990). Molecular dissection of mutations at the heterozygous thymidine kinase locus in mouse lymphoma cells. *Proc. Natl Acad. Sci. U.S.A.* **87,** 51–55.

Blazak, W. F., Los, F. J., Rudd, C. J., and Caspary, W. J. (1989). Chromosome analysis of small and large L5178Y mouse lymphoma cell colonies: Comparison of trifluorothymidine-resistant and unselected cell colonies from mutagen-treated and control cultures. *Mutat. Res.* **224,** 197–208.

Blazak, W. F., Stewart, B. E., Galperin, I., Allen, K. L., Rudd, C. J., Mitchell, A. D., and Caspary, W. J. (1986). Chromosome analysis of trifluorothymidine-resistant L5178Y mouse lymphoma cell colonies. *Environ. Mutagen.* **8,** 229–240.

Chen, T., Harrington-Brock, K., and Moore, M. M. (2002). Mutant frequencies and loss of heterozygosity induced by N-ethyl-N-nitrosourea (ENU) in the thymidine kinase (*TK*) gene of L5178Y/$Tk^{+/-}$-3.7.2C mouse lymphoma cells. *Mutagenesis* **17,** 105–109.

Chen, T., and Moore, M. M. (2004). Screening for chemical mutagens using the Mouse Lymphoma Assay. In *Methods in Pharmacology and Toxicology Optimization in Drug Discovery: In Vitro Methods* (Z. Yan and G. W. Caldwell, Eds.), pp. 337–352. Humana Press, Totowa, NJ.

Cimino, M. C., Tice, R. R., and Liang, J. C. (1986). Aneuploidy in mammalian somatic cells *in vivo*. *Mutat. Res.* **167,** 107–122.

Clark, L. S., Harrington-Brock, K., Wang, J., Sargent, L., Lowry, D., Reynolds, S. H., and Moore, M. M. (2004). Loss of P53 heterozygosity is not responsible for the small colony thymidine kinase mutant phenotype in L5178Y mouse lymphoma cells. *Mutagenesis* **19,** 263–268.

Clark, L. S., Hart, D. W., Vojta, P. J., Harrington-Brock, K., Barrett, J. C., Moore, M. M., and Tindall, K. R. (1998). Identification and chromosomal assignment of two heterozygous mutations in the *Trp53* gene in L5178Y $Tk^{+/-}$ 3.7.2C mouse lymphoma cells. *Mutagenesis* **13,** 427–434.

Clive, D., Glover, P., Applegate, M., and Hozier, J. (1990). Molecular aspects of chemical mutagenesis in L5178Y/$Tk^{+/-}$ mouse lymphoma cells. *Mutagenesis* **5,** 191–197.

Cross, S. M., Sanchez, C. A., Morgan, C. A., Schimke, M. K., Ramel, S., Idzerda, R. L., Raskind, W. H., and Reid, B. J. (1995). A p53-dependent mouse spindle checkpoint. *Science* **267,** 1353–1356.

Davies, M. J., Phillips, B. J., and Rumsby, P. C. (1993). Molecular analysis of mutations at the *Tk* locus of L5178 mouse lymphoma cells induced by ethyl methanesulphonate and mitomycin C. *Mutat. Res.* **290,** 145–153.

Dearfield, K. L., and Moore, M. M. (2005). Use of genetic toxicology information for risk assessment. *Environ. Mol. Mutagen.* **46,** 236–245.

Dobrovolsky, V. N., Shaddock, J. G., and Heflich, R. H. (2002). Mutagenicity of gamma-radiation, mitomycin C, and etoposide in the *Hprt* and *Tk* genes of $Tk^{+/-}$ mice. *Environ. Mol. Mutagen.* **39,** 342–347.

Duesberg, P., Rasnick, D., Li, R., Winters, L., Rausch, C., and Hehlmann, R. (1999). How aneuploidy may cause cancer and genetic instability. *Anticancer Res.* **19,** 4887–4906.

Helleday, T. (2003). Pathways for mitotic homologous recombination in mammalian cells. *Mutat. Res.* **532,** 103–115.

Honma, M., Hayashi, M., Shimada, H., Tanaka, N., Wakuri, S., Awogi, T., Yamamoto, K. I., Ushio-Kodani, K. N., Nishi, Y., Nakadate, M., *et al.* (1999). Evaluation of the mouse lymphoma *Tk* assay (microwell method) as an alternative to the *In vitro* chromosomal aberration test. *Mutagenesis* **14,** 5–22.

Honma, M., Momose, M., Sakamoto, H., Sofuni, T., and Hayashi, M. (2001). Spindle poisons induce allelic loss in mouse lymphoma cells through mitotic non-disjunction. *Mutat. Res.* **493,** 101–114.

Honma, M., Momose, M., Tanabe, H., Sakamoto, H., Yu, Y., Little, J. B., Sofuni, T., and Hayashi, M. (2000). Requirement of wild-type p53 protein for maintenance of chromosomal integrity. *Mol. Carcinog.* **28,** 203–214.

Hozier, J., Applegate, M., and Moore, M. M. (1992). *In vitro* mammalian mutagenesis as a model for genetic lesions in human cancer. *Mutat. Res.* **270,** 201–209.

Hozier, J., Sawyer, J., Clive, D., and Moore, M. M. (1982). Cytogenetic distinction between the TK^{+} and TK^{-} chromosomes in the L5178Y $TK^{+/-}$ 3.7.2C mouse-lymphoma cell line. *Mutat. Res.* **105,** 451–456.

Hozier, J., Sawyer, J., Moore, M., Howard, B., and Clive, D. (1981). Cytogenetic analysis of the L5178Y/$TK^{+/-}$ → $TK^{-/-}$ mouse lymphoma mutagenesis assay system. *Mutat. Res.* **84,** 169–181.

Ikui, A. E., Yang, C. P., Matsumoto, T., and Horwitz, S. B. (2005). Low concentrations of taxol cause mitotic delay followed by premature dissociation of p55CDC from Mad2 and BubR1 and abrogation of the spindle checkpoint, leading to aneuploidy. *Cell Cycle* **4,** 1385–1388.

Joseph, G., Grist, S., Firgaira, F., Turner, D., and Morley, A. (1993). Classification of mutations at the HLA-A locus by use of the polymerase chain reaction. *Environ. Mol. Mutagen.* **22,** 152–156.

Liechty, M. C., Crosby, H., Jr., Murthy, A., Davis, L. M., Caspary, W. J., and Hozier, J. C. (1996). Identification of a heteromorphic microsatellite within the thymidine kinase gene in L5178Y mouse lymphoma cells. *Mutat. Res.* **371,** 265–271.

Liechty, M. C., Hassanpour, Z., Hozier, J., and Clive, D. (1994). Use of microsatellite DNA polymorphisms on mouse chromosome 11 for *in vitro* analysis of thymidine kinase gene mutations. *Mutagenesis* **9,** 423–427.

Liechty, M. C., Scalzi, J. M., Sims, K. R., Crosby, H., Jr., Spencer, D. L., Davis, L. M., Caspary, W. J., and Hozier, J. C. (1998). Analysis of large and small colony L5178Y $Tk^{-/-}$ mouse lymphoma mutants by loss of heterozygosity (LOH) and by whole chromosome 11 painting: Detection of recombination. *Mutagenesis* **13,** 461–474.

Mailhes, J. B., Carabatsos, M. J., Young, D., London, S. N., Bell, M., and Albertini, D. F. (1999). Taxol-induced meiotic maturation delay, spindle defects, and aneuploidy in mouse oocytes and zygotes. *Mutat. Res.* **423,** 79–90.

Moore, M. M., Clive, D., Hozier, J. C., Howard, B. E., Batson, A. G., Turner, N. T., and Sawyer, J. R. (1985). Analysis of trifluorothymidine-resistant (TFTr) mutants of L5178Y/$TK^{+/-}$ mouse lymphoma cells. *Mutat. Res.* **151,** 161–174.

Moore, M. M., Mei, N., Chen, L., and Chen, T. (2005). Taxol induces mutations in the *Tk* gene of L5178Y/$Tk^{+/-}$ mouse lymphoma cells through a mitotic non-disjunction mechanism. *Toxicologist* **84,** 455.

Oshimura, M., and Barrett, J. C. (1986). Chemically-induced aneuploidy in mammalian cells: Mechanisms of biological significance in cancer. *Environ. Mol. Mutagen.* **8,** 129–159.

Sawyer, J. R., Moore, M. M., Clive, D., and Hozier, J. C. (1985). Cytogenetic characterization of the L5178Y $TK^{+/-}$ 3.7.2C mouse lymphoma cell line. *Mutat. Res.* **147,** 243–253.

Schiff, P. B., and Horwitz, S. B. (1980). Taxol stabilizes microtubules in mouse fibroblast cells. *Proc. Natl Acad. Sci. U.S.A.* **77,** 1561–1565.

Sen, S. (2000). Aneuploidy and cancer. *Curr. Opin. Oncol.* **12,** 82–88.

Storer, R. D., Kraynak, A. R., McKelvey, T. W., Elia, M. C., Goodrow, T. L., and DeLuca, J. G. (1997). The mouse lymphoma L5178Y $Tk^{+/-}$ cell line is heterozygous for a codon 170 mutation in the p53 tumor suppressor gene. *Mutat. Res.* **373,** 157–165.

Tarapore, P., and Fukasawa, K. (2000). *p53* mutation and mitotic infidelity. *Cancer Invest.* **18,** 148–155.

Wang, J., Chen, T., Honma, M., Chen, L., and Moore, M. M. (2007). 3′-azido-3′-deoxythymidine induces deletions in L5178Y mouse lymphoma cells. *Environ. Mol. Mutagen.* **48,** 248–257.

Zhang, L. S., Honma, M., Matsuoka, A., Suzuki, T., Sofuni, T., and Hayashi, M. (1996). Chromosome painting analysis of spontaneous and methyl methanesulfonate- induced trifluorothymidine-resistant L5178Y cell colonies. *Mutat. Res.* **370,** 181–190.